

Aero- Assist: A Guide Tool to Aid in the Generation of Surface Grids for CFD

A project present to
The Faculty of the Department of Aerospace Engineering
San Jose State University

in partial fulfillment of the requirements for the degree
Master of Science in Aerospace Engineering

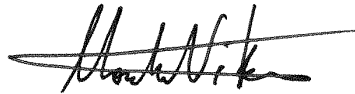
By

Omar E. Quijano

December 2013

approved by

Dr. Nikos Mourtos
Faculty Advisor



ABSTRACT

Achieving accurate Computational Fluid Dynamics (CFD) solutions that conform to physical reality requires physics-informed and high quality grids. In the conventional approach for generating these grids, there is a sense of artistry that lies in the expertise and diligence of the engineer. For engineers of all levels of experience, this is a time-

consuming and expensive process. The goal of this effort is to develop and demonstrate an innovative aerodynamic guide tool that is flow physics based, efficient (can explore a complete flight envelope in a timely manner), models important flow features, and facilitates the initial creation of effective CFD grids. The proposed approach is based on flow-physics-based aerodynamic methods, critical flow feature identification, uncertainty quantification, and the enhancement of an existing best practice expert system (BPX) for CFD.

This study will help develop an initial methodology that will demonstrate the feasibility of the proposed approach. Finally, a grid will be designed based on the recommendation from AeroAssist and benchmark with experimental data.

ACKNOWLEDGMENTS

I would like to express my gratitude to Dr. Mourtos for his continuous support and encouragement to finish my Master's; to my brother, Eduardo Quijano, for his continuous wisdom, patience, and love; to Dr. Papadopoulos for his guidance; to the NEAR Staff: Dr. Reisenthel and Mr. Lesieutre for their time, criticisms, ideas, and tools; and, to my father for his care. I offer my sincere appreciation for making AeroAssist a feasible idea.

The completion of this project could have not been plausible without the support and inspiration of other influential people in my life: Maureen Santos your endeavors and directness inspire me to achieve more.

Finally, I would like to thank my friend Eric Morales for correcting my grammar and helping express my ideas. You are all part of this project!

TABLE OF CONTENTS

LIST OF FIGURES.....	vii
LIST OF TABLES.....	ix
LIST OF ACRONYMS.....	x
LIST OF SYMBOLS.....	xi
I. INTRODUCTION.....	1
A. IDENTIFICATION OF THE PROBLEM.....	1
B. OBJECTIVE.....	2
C. BACKGROUND.....	3
D. AEROASSIST: INNOVATION OVERVIEW.....	5
II. LITERATURE REVIEW.....	6
III. AEROASSIST.....	9
A. GEOMETRY.....	10
B. SOLVER.....	11
C. FLOW FEATURE IDENTIFICATION.....	13
D. INFORMATION LAYER.....	14
E. AUGMENTED GEOMETRY.....	15
F. ENTITY CONSTRUCTION.....	15
G. MESH METRICS & MESH QUALITY.....	16
H. UNCERTAINTY ANALYSIS.....	17
I. DATABASE EXPERT SYSTEM.....	19
J. DATABASE MANAGEMENT SYSTEM.....	20
IV. PRELIMINARY VALIDATION.....	22
A. PRACTICAL IMPORTANCE.....	22
B. OBJECTIVE.....	23
C. METHODOLOGY.....	23
D. GEOMETRY.....	23
1. MODEL CONFIGURATION.....	23
E. ESI GRID GENERATION.....	25
F. AEROASSIST.....	26
1. GEOMETRY.....	26

2. SOLVER.....	27
3. INFORMATIONAL LAYER.....	28
G. VOLUME GENERATION.....	35
H. CODE COMPARISSON.....	38
I. BENCHMARK.....	41
V. CONCLUSION.....	43
VI. VISION.....	43
VIII. REFERENCES.....	45
IX. APPENDIX.....	47
A. AERODYNAMIC MODELING AND PREDICTION CAPABILITIES.....	47
B. BEST PRACTICES EXPERT FOR CFD.....	47
C. MESH AND QUALITY METRICS NUMERICS.....	48
D. OPTIMIZATION AND UNCERTAINTY QUANTIFICATION.....	49
E. POINTWISE.....	49
F. ESI.....	50
G. HYPGEN.....	50
H. OVERFLOW.....	50
I. TECPLOT.....	50
J. SAMPLE RAW DATA.....	51
K. ESI SAMPLE CALCULATION.....	55
L. OVERFLOW DATA EXTRACTION.....	56
M. EXPERIMENTAL DATA.....	57

LIST OF FIGURES

Figure 1. Various aerospace vehicles solutions created by AeroAssist solver (a) missile with fins, (b) military aircraft, (c) helicopter fuselage.....	2
Figure 2. Conventional CFD approach.....	4
Figure 3. AeroAssist enhanced CFD process.....	5
Figure 4. Functional modules of the AeroAssist.....	6
Figure 5. AeroAssist geometry preprocessing.....	11
Figure 6. AeroAssist flow feature identification model output.....	13
Figure 7. Detailed processes contained in the AeroAssist information layer module.....	14
Figure 8. Uncertainty and sensitivity analysis process.....	18
Figure 9. Separation line visualization based on laminar and turbulent criteria.....	19
Figure 10. Graphics output representaion of the AeroAssist process for the example of forebody flow physics.....	21
Figure 11. Sideview of original 3D forebody.....	24
Figure 12. Isometric view of extruded solid.....	24
Figure 13. Creation of butterfly mesh.....	25
Figure 14. Butterfly mesh projected onto surface.....	25
Figure 15. Complete mesh creation projected onto surface.....	25
Figure 16. AeroAssist geometry requirements.....	26
Figure 17. AeroAssist processed geometry.....	27
Figure 18. Pressure coefficient distribution.....	27
Figure 19. 2D forebody sideview.....	28
Figure 20. Nose tip linear regression.....	29
Figure 21. 2D plot shock location.....	29
Figure 22. 3D view shock location.....	30
Figure 23. X – pressure gradients.....	31
Figure 24. Y – velocity field.....	31
Figure 25. BPX GUI.....	32
Figure 26. Streamwise resolution refinement.....	33
Figure 27. Circumferential resolution refinement.....	34

Figure 28: AeroAssist surface grid.....	35
Figure 29: ESI geom volume grid.....	37
Figure 30: ESI volume side view.....	37
Figure 31: AeroAssist - hypgen volume grid.....	37
Figure 32: ESI residual history.....	39
Figure 33: Overflow residual history.....	39
Figure 34: ESI Mach sideview result.....	40
Figure 35: Overflow Mach isometric view result.....	40
Figure 36: Polar coordinate system.....	41
Figure 37: Pressure distribution comparison.....	42
Figure 38: Pressure distribution comparison.....	42
Figure 39 Conceptual GUI.....	44
Figure 40 BPX GUI.....	48
Figure 41: Pressure distribution for $\theta = 180^\circ$	55
Figure 42. Experimental results for $\theta = 180^\circ$	57

LIST OF TABLES

Table 1 Type of grids and output entities.....	15
Table 2: Flow conditions.....	27
Table 3. Sample raw data for one curve at $\psi = 6.25$	51
Table 4. ESI data extraction for $\theta = 180^\circ$	55
Table 5. OVERFLOW data extraction for $\theta=180^\circ$	56
Table 6. Experimental data extraction for $\theta = 180^\circ$	57

LIST OF ACRONYMS

CFD	=	Computational Fluid Dynamics.
BPX	=	Best Practice eXpert System.
CAD	=	Computer – Aided Design.
CAE	=	Computer Aided Engineering.
LLNL	=	Lawrence Livermore National Laboratory.
IGES	=	Initial Graphic Exchange Specification.
CAPRI	=	Computational Analysis Programming Interface.
C3LIB	=	Chimera Components Connectivity Library.
CGT	=	Chimera Grid Tools.
OVERFLOW	=	OVERset grid FLOW solver.
SAGE	=	Self Adaptive Grid code.
UQ	=	Uncertainty Quantification.
NEAR	=	Nielsen Engineering & Research, Inc.
SJSU	=	San Jose State University.
°	=	Degrees.
GUI	=	Graphical User Interface.
UAV	=	Unmanned Aerial Vehicle.

LIST OF SYMBOLS

α	=	Angle of attack, °.
β	=	Side slip angle, °.
M	=	Mach number
Re	=	Reynolds number
C _p	=	Pressure coefficient
σ	=	Semivertex angle, °.
φ	=	Modified Shock wave angle, °.
FTSHK	=	Maximum nose shock wave angle, °.
Δs	=	Grid Spacing
v	=	Y- velocity.
Z _{min}	=	Y=0, minimum Z surface profile.
Z _{max}	=	Y=0, maximum Z surface profile.
P	=	Pressure.
P _∞	=	Freestream pressure.
q _∞	=	Dynamic pressure.

I. INTRODUCTION

In the field of Computational Fluid Dynamics (CFD), a certain degree of art is still required to obtain numerical simulations that conform to physical reality. Much effort has been spent in designing technology that can automatically create computational meshes—some of these technologies will be examined in the literature review section. The issue with some of these methods is that they define quality in terms of geometry and lack the accuracy to capture gradients in the near flow field of the surface. Too coarse of a mesh causes sharp gradients in the flow field to suffer from numerical diffusion, where sudden changes in the fluid properties behavior are unrealistically “smeared.”¹ The

balance between physical fidelity and computational expense is a problem that CFD practitioners must address by intuition and experience. The scope of this project is to demonstrate the feasibility of a preliminary Aero-Guide tool (hereinafter AeroAssist) to help produce an *Intelligent Surface Grid*. This entails Aerodynamic Feature Identification and knowledge extraction from an expert system to create augmented geometry CAD entities or adapt the surface grid to aid the surface grid generation process.

A. IDENTIFICATION OF THE PROBLEM

Current grid creation and refinement technologies require iterative CFD calculations to produce an acceptable surface mesh.² This iterative process makes it expensive to achieve a converged CFD solution, and manually refining the surface becomes time consuming for complex Aerodynamic Analysis. Hence, for production engineering applications, time and available computational hardware may force the “acceptable” mesh to be of significantly lower quality than the optimum mesh, resulting in increased computational cost with lower solution fidelity.³

The following figure identifies flow features, which must be taken into account when generating CFD meshes. These include regions of strong pressure gradient, onset flow separation, and convected vortices affecting downstream subcomponents.

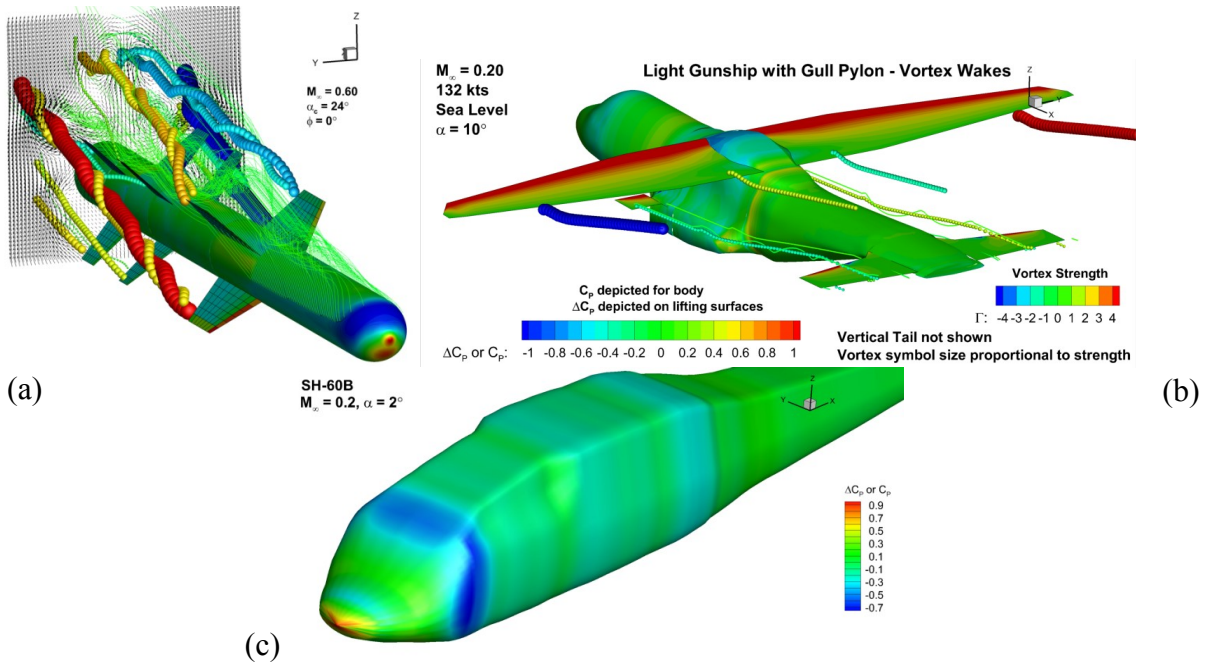


Figure 1. Various aerospace vehicles solutions created by AeroAssist solver (a) missile with fins, (b) military aircraft, (c) helicopter fuselage.

B. OBJECTIVE

The objective of the proposed project is to develop and demonstrate an innovative Aerodynamic Guide Tool (AeroAssist) that is computationally efficient, models important flow features, and aids the creation of economical and “accurate” CFD grids. The proposed AeroAssist will be based on three technologies: (i) physics-based aerodynamic methodologies, which identify important flow features quickly over large ranges of flow conditions, (ii) rigorous uncertainty quantification and sensitivity analysis, and (iii) a best practices expert system for CFD. The AeroAssist, described herein, will aid CFD users to generate flow-physics-based high-quality surface and volume grids, thus reducing the time currently required to obtain accurate CFD results.

C. BACKGROUND

The conventional process required to achieve quality CFD solutions is depicted in Figure 2. This process is expensive, because iterative surface grid refinements are required to increase the flow solution accuracy, which is time intensive. Geometries are usually transmitted from the CAD system, which are “no good” for the grid generator. The grid generator needs smooth closed solid geometry. It can take a week (or more) of interaction with the CAD output (sometimes by hand) before the process can begin.³ For companies and educational institutions with limited computational resources, time and hardware constraints may significantly lower the quality of the mesh(es). Although larger organizations may have the means and flexibility of generating high-resolution grids, this approach is inefficient and can potentially cause other numerical problems. In addition, for many recent graduates or engineers with limited experience, understanding mesh metrics and being able to anticipate mesh quality requirements (e.g., accurately capturing surface or flowfield gradients) are challenging tasks. Thus, the conventional CFD process still requires a considerable degree of art to obtain solutions that can be critically judged to conform to physical reality.

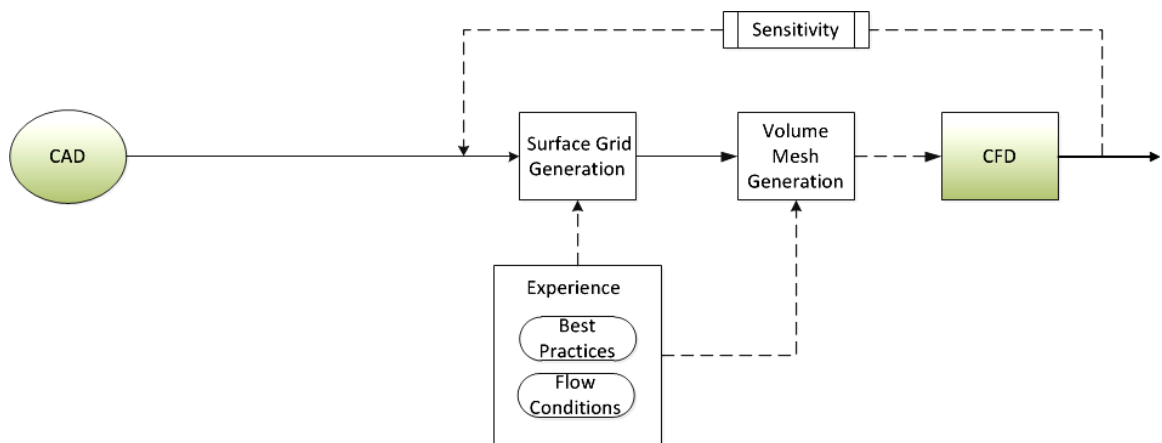


Figure 1. Conventional CFD approach.

In order to achieve a solution that conforms to physical reality, there must exist a balance between physical fidelity and computational expense. In the conventional CFD framework, practitioners address this issue by intuition and experience. This experience and intuition is not always general knowledge, nor is it transmitted to other engineers. The proposed approach, depicted in Figure 3, will identify important regions of the flow, process them, and add these features to the CAD model or adapt the surface grid. These additional CAD entities will assist the CFD user in creating higher quality grids the first time, i.e., before any CFD solution has been run. Detail of the AeroAssist approach is given in Figure 4.

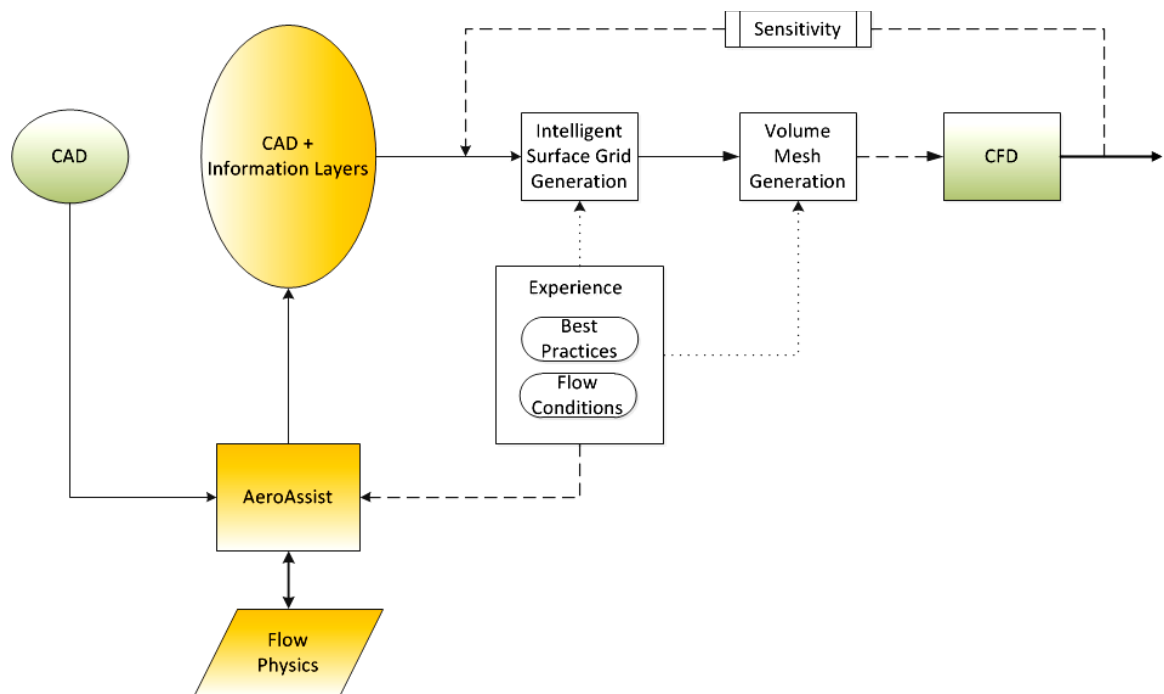


Figure 1. AeroAssist enhanced CFD process.

D. AEROASSIST: INNOVATION OVERVIEW

The AeroAssist will integrate specific tools to guide the CFD user tasked with designing and/or modeling vehicle(s) for aerodynamic analysis. The overall advantages of AeroAssist are:

- i. Fast representation of the flow features for any given geometry.
- ii. Flow feature identification over the flight envelope.
- iii. Identification of flow regime(s) requiring new or updated mesh(es).
- iv. Reduction of the number of iterations and time with respect to the conventional CFD approach.
- v. Sensitivity and uncertainty analyses related to input parameters, flow conditions, and solver. Grid-type independence/neutrality.
- vi. Accuracy of the solution would be increased and can be the basis for performance to other engineering disciplines.
- vii. Ease of use by both CFD experts and engineers with limited experience.

Details of the AeroAssist components are given below, followed by a description of each module in Section III.

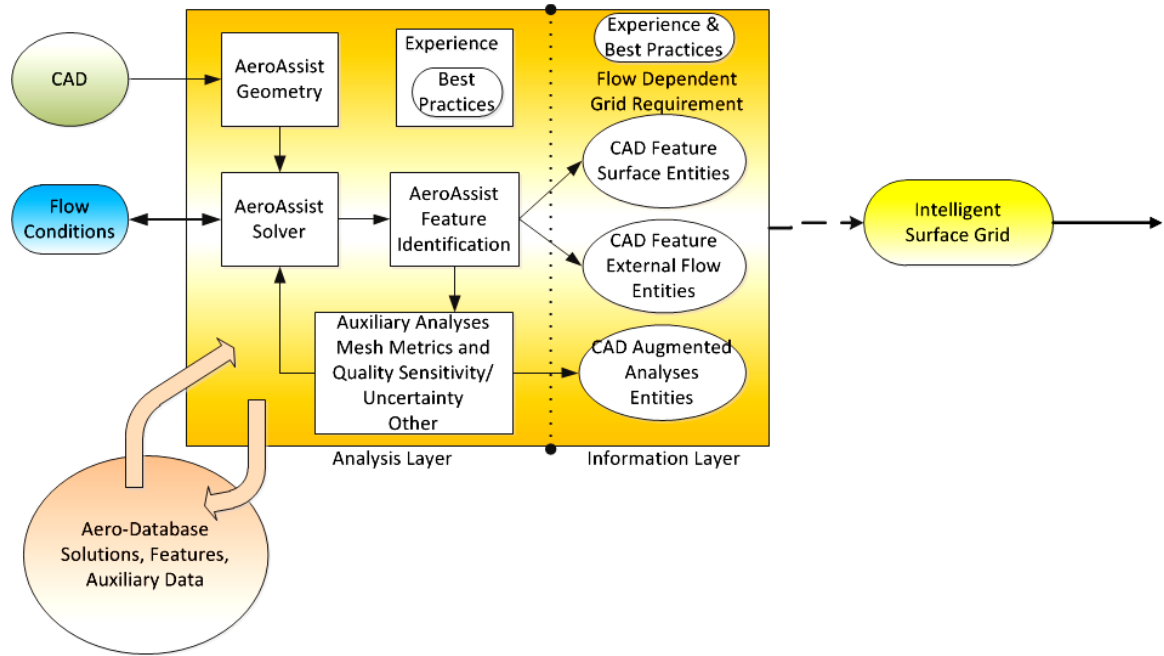


Figure 1. Functional modules of the AeroAssist.

II. LITERATURE REVIEW

CFD has become an indispensable design tool in the aerospace industry. High fidelity and precision CFD results offer considerable independence from expensive testing process and experimental methods like wind tunnel testing or flight testing allowing early prediction of design optimization.⁷ With current technology, such as supercomputers, better solutions can be achieved; however, there is ongoing research in the reduction of time and cost in the CFD process. The following is a summary of some of these technologies with an explanation as to why AeroAssist is different and innovative.

A Software Demonstration of “rap” developed by LLNL. Rap is part of the Overture overlapping grid framework. It is a software tool for preparing CAD geometries (IGES files) for mesh generation and creating overlapping meshes.⁸ In other words, it is a tool

that helps the user go from CAD to a volume grid. Rap still needs further work to go directly from CAD to a water tight surface because errors can span if the underline CAD geometry is ill defined; meaning, there are missing or duplicated surfaces, or if the tolerance threshold is exceeded. The user can then spend time debugging the problem by either iterating the CAD geometry or manipulating the grid.

CAPRI is a software building tool-kit that refers to two ideas: (i) A simplified, object-oriented, hierchical view of a solid part integrating both geometry and topology definitions, and (ii) programming assess to this part or assembly and any attached data.⁹ CAPRI is a lightweight application, only requiring libraries, and provides a gateway between Computer Aided Engineering (CAE) applications with the CAD system . CAPRI, however, has a major drawback in that it is a commercial product. Furthermore, the tessellation themselves are not directly suitable as a flow mesh and thus must be used as a driver for a more flow oriented mesher.¹⁰

CEASIOM a software system developed in the EU to generate stability and control data for conceptual and preliminary aircraft design using a choice of numerical methods of varying fidelity.¹¹ The CEASIOM framework integrates discipline-specific tools, with the main focus on aircraft design, to go from CAD to an adaptive-fidelity CFD solution. Although CEASIOM offers a complete solution to the stated problem, it requires engineer interaction for mesh development and fidelity, lacks automation, it is an unstructured solver, and the turn-around data can be deceptive due to the lack of robustness from the models and grids.

In the Overset Structure Grid Generation, process advances have been made towards

automated and efficient domain connectivity by means of using newly developed libraries of domain connectivity function called Chimera Components Connectivity Library (C3LIB). These libraries are incorporated into the Chimera Grid Tools (CGT) software package. Chimera Grid Tools is a collection of software tools created specifically for the efficient pre-processing and post-processing of structured overset grid computations.¹² There are over 100 scripted macros that can be invoked which speed the grid generation process. This approach, however, is not fully automated. Scripts need to be manually created the first time and require modification if a topological change occurs in the geometry.¹²

CART3D is a high-fidelity inviscid analysis package for conceptual and preliminary aerodynamic design. The package is highly automated so that geometry acquisition and mesh generation can usually be performed within a few minutes on most current desktop computers.¹³ Its adjoint algorithm allows the grid to be refined based on a certain threshold to obtain an optimum mesh for a particular flow solution. Although CART3D is a great tool, it can be resource intensive and the process from CAD to grid can be time consuming.

There exist many tools that can reduce the grid generation process, but none are as fast, modular, user friendly, and economical as AeroAssist.

III. AEROASSIST

The overall objective of this work is to pioneer an innovative tool, AeroAssist, that utilizes physics-based predictions of flow features to guide the CFD user during the

initial mesh generation process.

The objective of the proposed project is to demonstrate the feasibility of an Aerodynamic/Fluid Dynamics Guide Tool to assist the CFD user in generation of an *Intelligent Surface Grid*. An *Intelligent Surface Grid* is an economical surface grid with sufficient fidelity, based on mesh metrics and mesh quality, and its physics. The specific objectives of the proposed work are enumerated as follows:

- i. Identify on-surface and near-surface regions of the flow which require modeling to improve the accuracy of the CFD solutions.
- ii. Demonstrate the ability to identify flow regimes and/or ranges where either new or additional grids are required to maintain CFD solution fidelity due to flow condition sensitivity.
- iii. Generate physics-augmented “CAD layers” containing important flow feature-derived information for creation of an *Intelligent Surface Grid*.
- iv. Define guidelines and requirements for sensitivity and uncertainty analysis for robust grid generation.
- v. Investigate the integration of the BPX expert system with user knowledge through the use of the AeroAssist, and personal CFD experience.
- vi. Identify the requirements to develop a software tool.

The specific questions the project will aim to answer to determine the feasibility of the proposed innovation are as follows:

- a. Does the proposed AeroAssist tool (a) increase initial solution accuracy, and (b) reduce the amount of time, effort, and computational resources to complete the

aerodynamic analysis?

- b. Can the AeroAssist tool integrate the identification of flow features, geometrical metrics, operational variations, uncertainty and expert system into one software package?

Successfully answering these questions while addressing objectives (i)-(vi) will provide the foundation for a tool that can intelligently guide the initial creation of computationally economical surface grids for complete military aircraft, missiles, and wetted external components.

A. GEOMETRY

The AeroAssist Geometry module will efficiently generate a representation of the vehicle. The conventional grid generation process manually manipulates the CAD model to remove unwanted objects that represent unnecessary features. Thus, a CAD geometry imported from IGES files or native CAD files (ACIS, CATIA, STEP, SolidWorks) is first “cleaned-up” and simplified for the AeroAssist solver. For this project, Pointwise will be used to import and heal CAD models. Through scripting, the model will be manipulated to generate a triangulated geometry of subcomponents and create input files required by the AeroAssist. This process is graphically illustrated below:

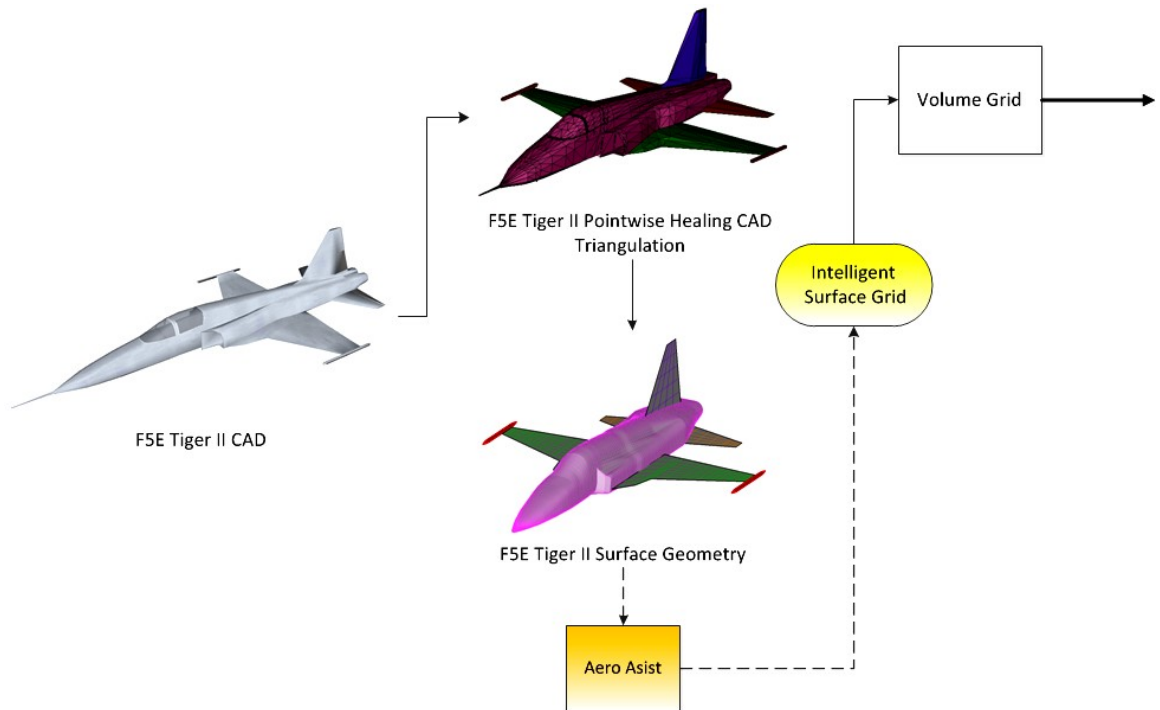


Figure 1. AeroAssist geometry preprocessing.

B. SOLVER

The AeroAssist solver is a fast-running intermediate-level flow solver. The aerodynamic prediction tool will be based on subsonic and supersonic panel methods and on classical aerodynamic theory³. The flow solver methodology, captured flow phenomena, and aerodynamic prediction applications are summarized below.

Methodology:

- Non-linear panel-method based
- Circular and noncircular bodies
- Arbitrary planform/fin layout
- High- α body and fin vortex wakes

- Rotational rates, nonuniform flow
- Vortical transport
- Separated body and fin flow
- Shock expansion and Newtonian pressure calculation methods
- Boundary layer separation criteria

Flow phenomena:

- Mach number
- High angle of attack
- Arbitrary roll angle
- Fin and control surface deflection
- Vortex wake effects including swirl.

Aerodynamic prediction applications:

- Preliminary design, trade-off studies, optimization;
- Generation of large database for flight Simulation;
- Augmenting wind tunnel and CFD databases;
- Detail load distribution and flow characteristics; and
- Surface pressures and lifting surface loading.

Future work will provide AeroAssist with additional fast-running aerodynamic and fluid dynamic prediction methods which capture flow phenomena not modeled in the current flow *solver*. For example, these could include boundary layer prediction codes.

C. FLOW FEATURE IDENTIFICATION

This module will identify flow features predicted by the AeroAssist *solver* which are important to high-quality grid generation. Flow features which influence surface gridding, include: regions of strong pressure gradient, flow separation, and vortices affecting downstream surfaces (subcomponents). This module will generate feature specific “elements,” which will be processed in the Information Layer (Figure 4) to create CAD feature entities or self adapt the surface topology. Identified “elements” will include, but are not limited to: regions of high pressure gradients, flow separation lines, and vortex wake paths. These elements will be supplied as inputs to auxiliary analysis modules, such as sensitivity and uncertainty analyses (described in H). By means of example, flow features predicted by the *solver* for a forebody at high angle-of-attack are shown below:

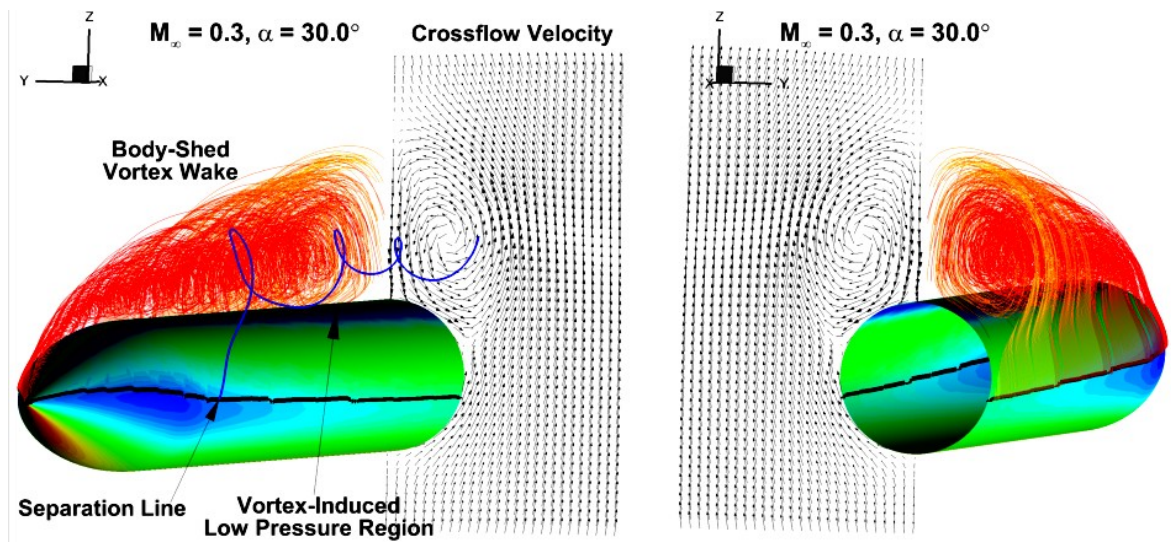


Figure 1. AeroAssist flow feature identification model output.

D. INFORMATION LAYER

The AeroAssist Information Layer uses the information provided by the Flow Feature Identification module to create physics-enhanced CAD entities or to self adapt the grid. These enhanced CAD entities contain attributes describing geometry to aid the user in creating higher-quality grids. The self adaptive surface definition contains attributes describing mesh quality metrics designed to generate a higher-quality surface grid. The created CAD entities and self adaptive topology are based on the extracted flow features, a Best Practices eXpert system for CFD named BPX,⁴ and flow feature uncertainty and sensitivity information with respect to various flow conditions and modeling parameters.

A schematic can be seen below:

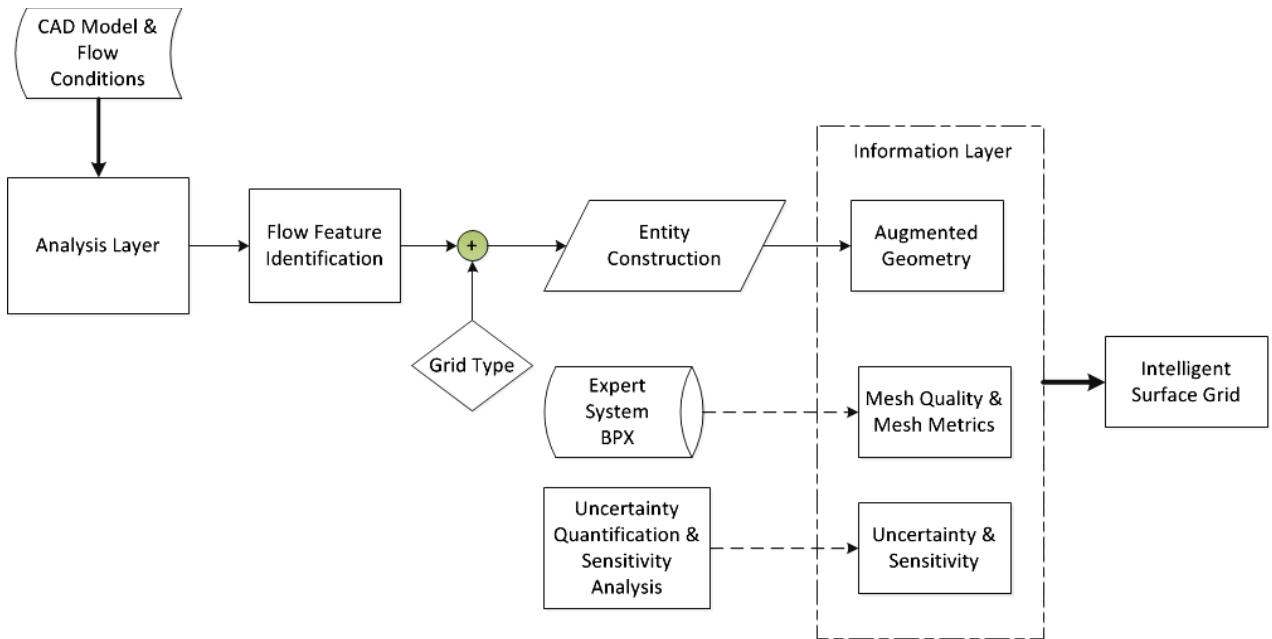


Figure 1. Detailed processes contained in the AeroAssist information layer module.

E. AUGMENTED GEOMETRY

As a result of the AeroAssist Feature Identification Module, the CAD entities generated will provide the CFD user with the location of important flow features. This module provides an *a priori* definition of a mesh for a given computational analysis, independent of grid type. The following table is a summary of the type of grids being considered and how they affect the design process. The outputs of mesh quality metrics and sensitivity analysis are also indicated to reduce the analysis error.

Table 1 Type of grids and output entities.

Grid Type	Flow Identification	Augmented Geometry	Quality, Metrics & Sensitivity	Topology Recommendation
Unstructured	Location of flow feature (Points and Lines)	ConcentrationCurve	Area of increased Resolution, Min/Max	Element Type
Overset		Quadrilateral (Patch)		Cartesian Box
Abutting				Topology

F. ENTITY CONSTRUCTION

The Entity Construction process is the main input for the Information Layer. The following defines the created entity and describes how it is processed to create an Augmented Geometry for each grid type.

Unstructured Grids:

1. Concentration curve(s) or sets of points that define the flow feature.
2. The line is projected onto the surface
3. Recommendation: increase grid resolution on the specified curve to capture the flow phenomena.

Overset Grids:

1. Concentration curve(s) or sets of points that define the flow feature.

2. A quadrilateral is constructed from the flow feature and is subsequently projected onto the surface.
3. Recommendation: creation a cartesian box(es) with increased resolution to capture the different flow phenomena.

Abutting Grids:

1. Concentration Curve(s) or set of points that define the flow feature.
2. A quadrilateral is constructed from the flow feature and projected onto the surface.
3. Recommendation: overall grid topology recommendation based on the anticipated flowfield characteristics.

G. MESH METRICS & MESH QUALITY

The purpose of this module is to reduce grid generation uncertainty over a wide range of flow conditions. This module will contain visual and statistical guidelines to help the user generate higher quality and “accurate” CFD grids. The following is a summary of different analyses to quantify the level of accuracy for different grid types. This module will also generate grid recommendations for accuracy and efficiency.⁵⁻⁶

Unstructured Grids:

Different element types include tetrahedral, hexahedral, and/or prismatic elements. Grid quality metrics depend on whether the mesh is fully tetrahedral versus hybrid, e.g., of tetrahedral-prismatic type.

Area of refinement samples: Boundary layer, spanwise-stretching, separated flow transition, trailing-edge refinement, etc.

Structured Grids:

A self adaptive grid code will be used to aid in the generation of the surface grid. It will focus on grid topology, element type, aspect ratio, skewness, and orthogonality measures.

Area of refinement samples: leading–edge, trailing–edge, area of high gradients, etc.

The final Grid Recommendation from this module will be based on the following:

1. Best practices and specific guidelines to assist in grid generation
2. Mesh metrics and mesh quality metrics generated by AeroAssist.
3. The output from augmented geometry module.

H. UNCERTAINTY ANALYSIS

In the conventional CFD practice, it is difficult to assert the degree of accuracy in a system that contains levels of errors and uncertainties.¹³ Thus, it is important to develop methods that perform error and uncertainty analyses. This module will increase the level of robustness of the grid generation process by minimizing the sensitivity to parameters whose value is modeled as uncertain. The anticipated result will be a reduction of the cost associated with traditional iterations. Properly quantified uncertainties may also provide the user with a more detailed understanding of the flow variable sensitivities.

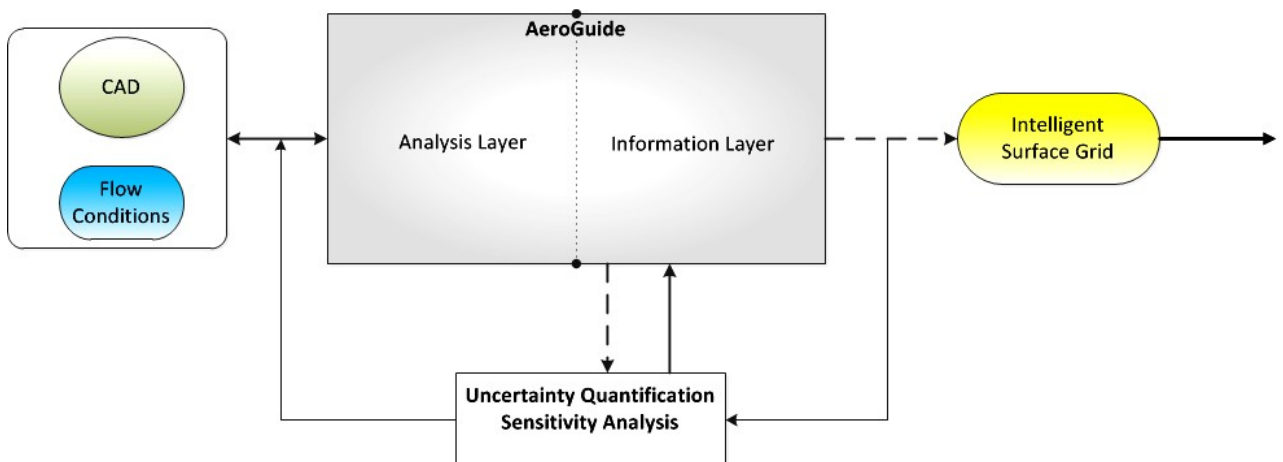


Figure 1. Uncertainty and sensitivity analysis process.

Uncertainty Quantification (UQ) for AeroAssist predictions will involve several steps, (i) the identification of which of the input variables are treated as uncertain, (ii) a quantitative characterization of the aleatory and epistemic input uncertainties, and (iii) a propagation scheme of these uncertainties. Ensemble statistics of the predicted flow features will be computed efficiently using polynomial chaos expansions.¹⁴

Aleatory uncertainty is associated with quantities such as flow properties; epistemic or model-form uncertainty is associated with lack of knowledge. An example of a source of epistemic uncertainty in the AeroAssist Solver is illustrated in Figure 9, in which the difference between computed laminar and turbulent separation lines can be used as an input uncertainty interval in the UQ computation.

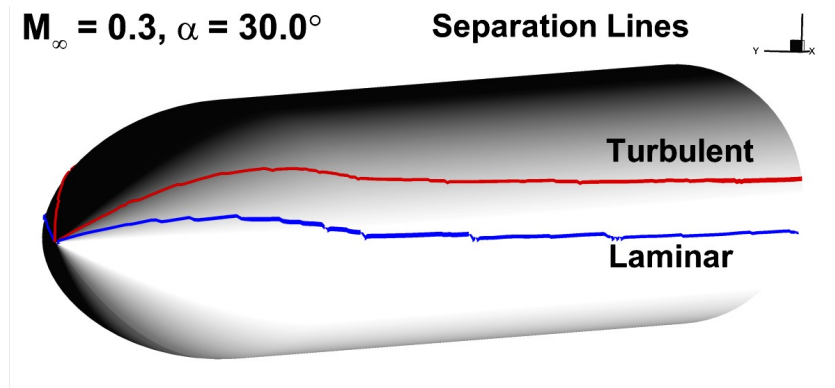


Figure 1. Separation line visualization based on laminar and turbulent criteria.

I. DATABASE EXPERT SYSTEM

In CFD there is a sense of artistry that lies in the expertise and diligence of the engineer who manages the countless details that go into a typical CFD simulation. It is important to utilize and capture this knowledge to produce higher quality grids and to

lower cost. NEAR's best practice system called BPX provides expert knowledge in the use of CFD codes to users, developers, and technology managers.⁴ The system enables CFD users to generate high-quality CFD solutions based on specific guidelines, code selection, input preparation, *grid generation*, parameter specification, result interpretation, verification, and validation. This expert system adds another layer of accuracy to the grid generation process and facilitates knowledge transfer to engineers with minimal experience. BPX is an existing tool which will be embedded in the AeroAssist and will be further enhanced in the future.

J. DATABASE MANAGEMENT SYSTEM

A database management system is part of the vision for AeroAssist, which will archive AeroAssist generated information, CFD grids and results information, lessons-learned, and will modify, analyze, and extract information from BPX. The creation of a hierarchical database will benefit users of all levels of experience by maintaining important information and making knowledge readily available. Knowledge in this context is defined as a CFD user's personal experience, recommendations, lessons learned, technical documentation, and data.

The proposed AeroAssist tool has the potential to assist the engineer with any level of CFD experience, in making decisions that will lead to more accurate computational results in less time and at lower cost by reducing the number of iterations, uncertainty and error. The figure below is a notational representation of one of the graphical product generated by AeroAssist.

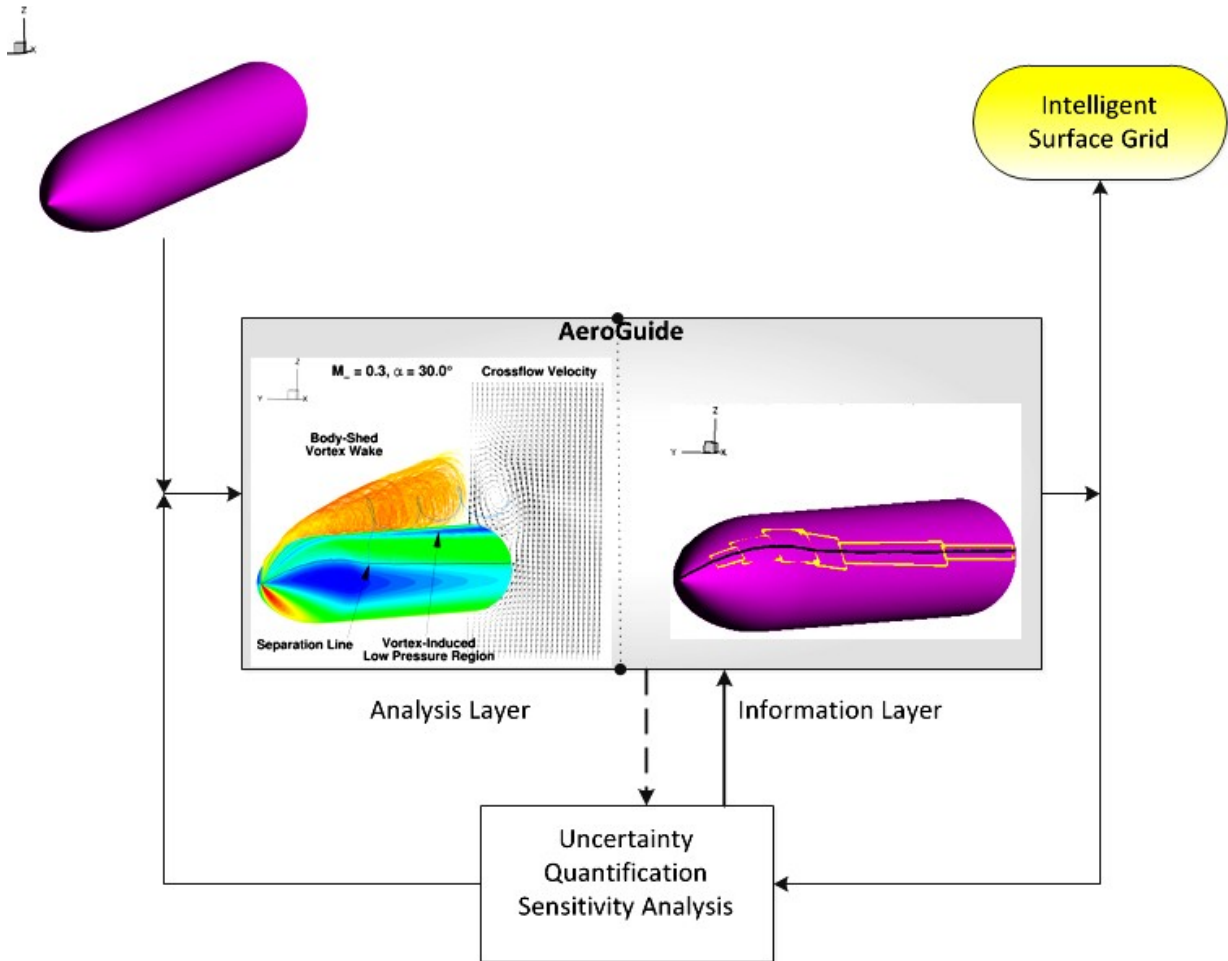


Figure 1. Graphics output representaion of the AeroAssist process for the example of forebody flow physics.

IV. PRELIMINARY VALIDATION

A supersonic forebody validation given by ESI-CFD will be used to compare the methodology behind AeroAssist. Even though the purpose of AeroAssist is not to obtain a CFD solution, it would be used to guide the mesh creation for the CFD solver OVERFLOW. OVERFLOW will be used to compare the pressure coefficient at the center-line because CFD-Fastran from ESI is no longer available. Two grids will be compared: i) grid created by an undergraduate student at SJSU using ESI, ii) and ii) the grid generated by using AeroAssist.

A. PRACTICAL IMPORTANCE

The study of supersonic flow is of high importance for a variety of problems, such as: the design of a high-speed plane, missile, rocket, etc. “For many years, steady development in numerical and theoretical methods has been pursued to accurately capture supersonic flow field characteristics.”¹⁵ Building a full scale model to test is costly, thus having a reliable tool to create dynamically similar environments becomes invaluable. CFD software is a useful tool that captures the design and development of the flow characteristics over a body; hence, this validation study presents CFD-FASTRAN and Overflow results for supersonic flow over a forebody of a given shape. Furthermore, this experiment is designed to compare the grid generation process and to accurately validate the predictive method against experimental data.

B. OBJECTIVE

To compare the surface grid for a given forebody and validate it by comparing the surface pressure data obtained from CFD-FASTRAN and OVERFLOW with the experimental data for a range of azimuthal locations at given cross sections.

C. METHODOLOGY

ESI-group CFD software package and OVERFLOW are employed to obtain the results for the pressure data points for a range of azimuthal locations at given cross section by first creating the entire 3-D domain and surface mesh in CFD-GEOM and Pointwise, grid generator packages. Secondly, the flow field is computed using CFD-FASTRAN and OVERFLOW, the solver packages. Lastly, the results were seen in CDF-VIEW and Tecplot, the solution packages.

D. GEOMETRY

1. MODEL CONFIGURATION

The model configuration for this study is a forebody which has analytically defined cross-sections and which are based on a parabolic-arc profile having a 20° half angle at the nose. The surface of the forebody is generated from the following parametric equations:

$$r_1 = \frac{1}{1.25 - .25 \cos(2\psi) + .13174[\cos(\psi) - \cos(3\psi)]}$$

$$r_2 = \left(1 - \frac{x}{2l}\right) \frac{x}{l} \tan(20^\circ)$$

$$\frac{y}{L} = r_2 \left[1 + (1.35r_1 - 1) \sin^2 \left(\frac{\pi x}{l} \right) \right] \sin(\psi)$$

$$\frac{z}{L} = r_2 \left[1 + \left(1.35r_1 - 1 + \frac{.35}{\cos(\psi)} \right) \sin^2 \left(\frac{\pi x}{l} \right) \right] \cos(\psi)$$

Where, r_1 , r_2 , x , l , L , ψ are dimensionless parametric variables used to describe the surfaces. The values for r_1 , r_2 , l , and L are kept constant at 1 unit, while the value for ψ are varied by .25 increments from 0 to 6.25 units. There is a total of 51 points that defined a curve for each increment of ψ (see appendix G for sample data set). There were a total of 25 curves developed to generate the 3-D forebody. After generating all the data points, the file was transferred to CFD-GEOM where the solid surfaces were generated (Figure 11). In order to complete the forebody, the original solid was extruded

to 5 characteristic lengths (see figure 12)

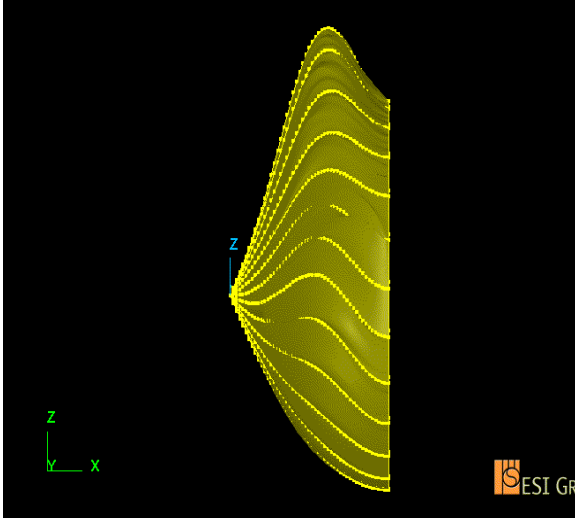


Figure 2. Sideview of original 3D forebody.



Figure 3. Isometric view of extruded solid.

E. ESI GRID GENERATION

The grid on the surface of the body was done only for a half-surface due to symmetry in the plane $y = 0$. The first step was to generate a butterfly mesh around the nose of the forebody. A butterfly grid was chosen because it has the best grid quality in terms of orthogonality and mesh density. After the mesh was created, it was projected onto the surface of the solid. For the remaining surface of the forebody, an h-mesh is used because the curvature is less complicated and the flow conditions do not vary as much as the nose.

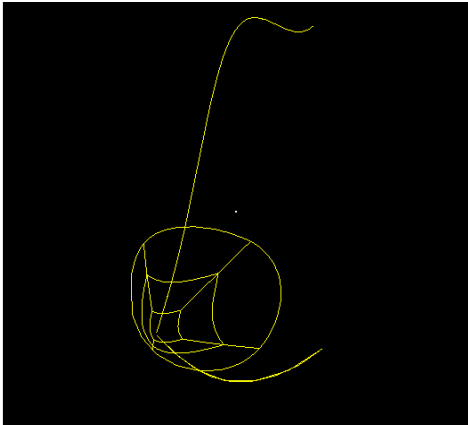


Figure 4. Creation of butterfly mesh.

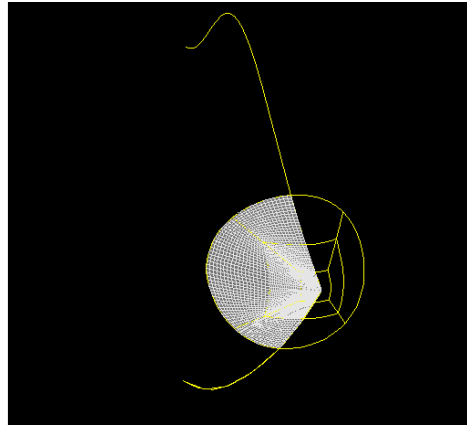


Figure 5. Butterfly mesh projected onto surface.

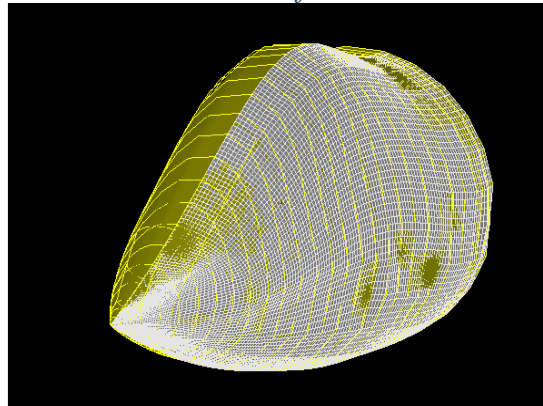


Figure 6. Complete mesh creation projected onto surface.

F. AEROASSIST

Following the logic of the AeroAssist process, the solid model obtained from the equations is decomposed into geometry readable by the solver.

1 GEOMETRY

The solver requires half-body data, axial stations (X), bottom meridian coordinates (Z_{min}), and top meridian coordinates (Z_{max}). For each cross-section; X , the values of Y and Z are extracted from the model and arranged in block format. The following image depicts the vertical coordinates of an arbitrary body cross-section and the outcome from

the AeroAssist geometry processing tool.

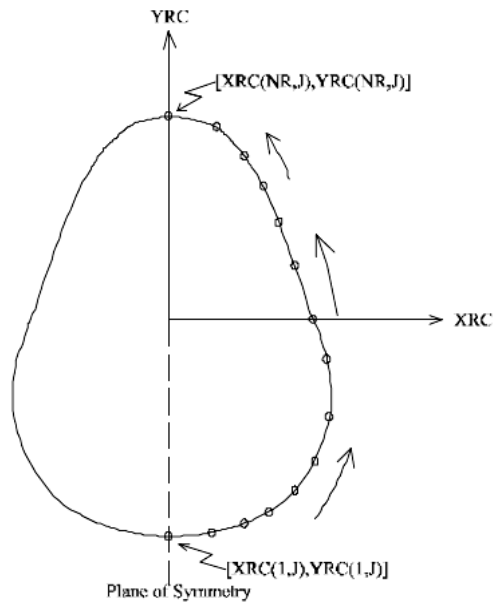


Figure 7. AeroAssist geometry requirements.

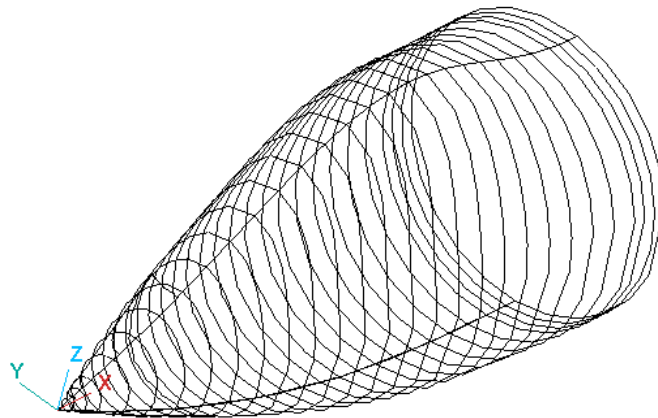


Figure 8. AeroAssist processed geometry.

2 SOLVER

The following table shows the flow conditions, separation criteria, and sample output for this validation:

Table 1: Flow conditions.

Property	Value
Separation	Laminar
M	1.70
α	-5.0°
β	-0.04°
Re/L	2.33E06

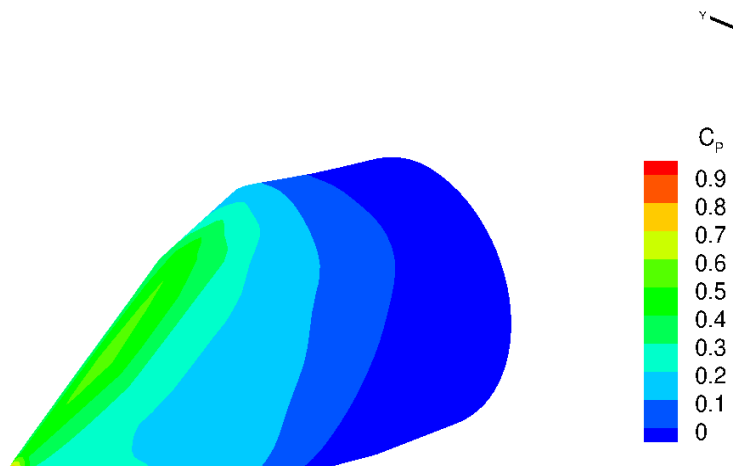


Figure 9. Pressure coefficient distribution.

The solver provides some basic physics that the information layer will interpret to design an *intelligent surface grid*, which will be physics-based and will have geometric-qualities.

3 INFORMATIONAL LAYER

For this particular case, the flow feature of interest would be the bow-shock caused by the conical body. At $\alpha = -5^\circ$, there is not a separation line to estimate and there is not a wake to re-project to the surface. To estimate the bow-shock, the user must specify the maximum nose shock wave angle in degrees: the first 9 points that define the nose are taken to be linear.

Forebody Side-View

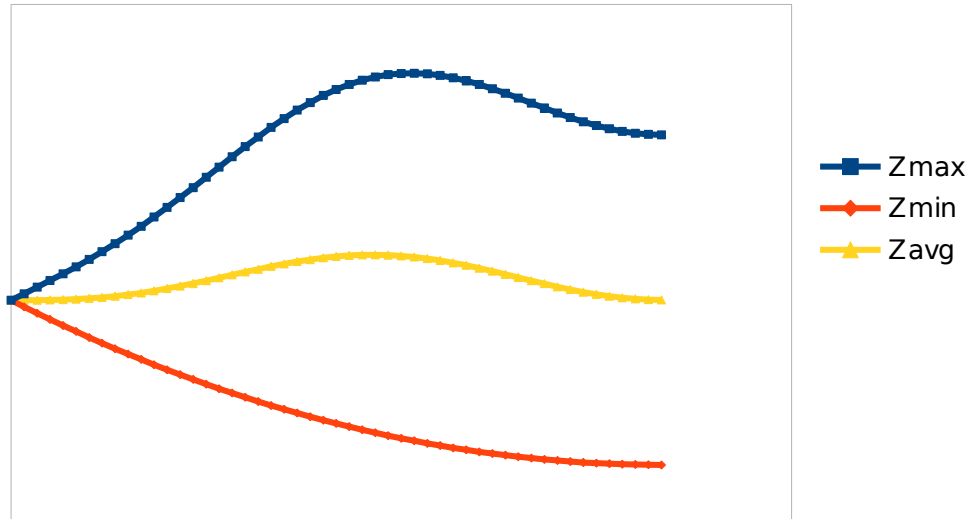


Figure 10. 2D forebody sideview.

Estimating Cone Semivertex Angle

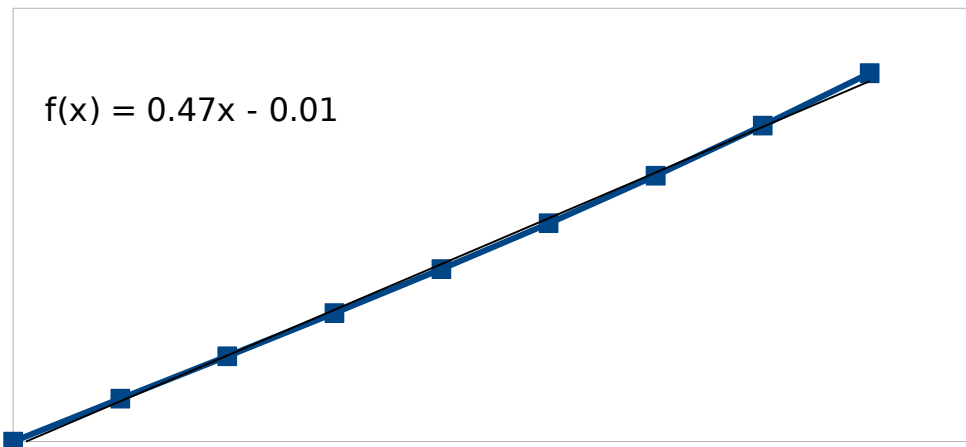


Figure 11. Nose tip linear regression.

Based on the linear equation obtained from excel, the estimated cone semivertex

angle, $\sigma = 25.4^\circ$. Using reference 16 the shock wave, θ , is estimated to be 49.2° . This variable, FTSHK, is inputted into the *Information Layer* to estimate the modified shock location, ϕ . A 2D and 3D view of the shock location can be seen in the figures below:

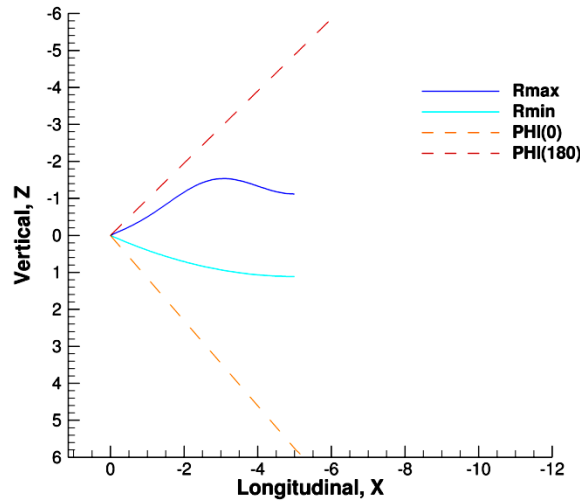


Figure 12. 2D plot shock location.

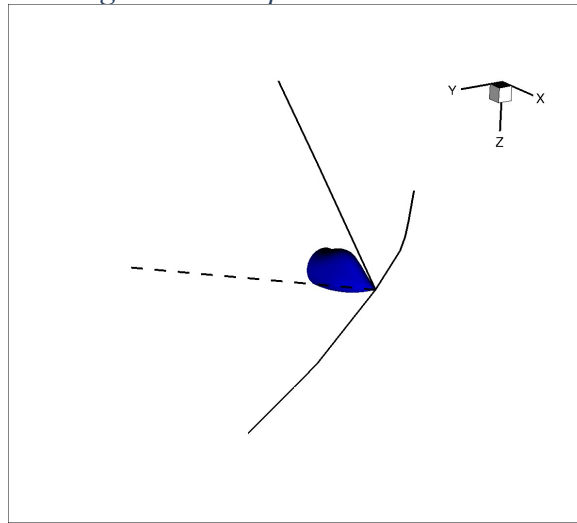


Figure 13. 3D view shock location.

Given the shock estimate, one can observe from Figure 19 the extent the volume grid has to grow to capture the shock, which is roughly 6 units. The information layer can

then provide augmented CAD entities (lines), as seen in Figure 20, which will aid the user in refining the surface and volume grid. However, the question: “What is the optimum number of points that must be added?” Still remains unanswered. There are three methodologies that the user can pick from: i) based on the solver estimate of pressure gradients, ii) purely based on best practices, or iii) based the Δs in best practices and use the pressure gradient to estimate the regions that require higher point density. For the first methodology, AeroAssist will estimate the pressure gradients on the surface and output the result visually. The user can then use this information to define the surface topology and resolution. The following figures show the pressure gradient on the surface and the v velocity field, respectively. One will observe on figure 21 the need for more points near the nose-tip and before the flat surface of the body. Figure 21 shows that the flow is moving along the body (attached); meaning, there is no vorticity effect.

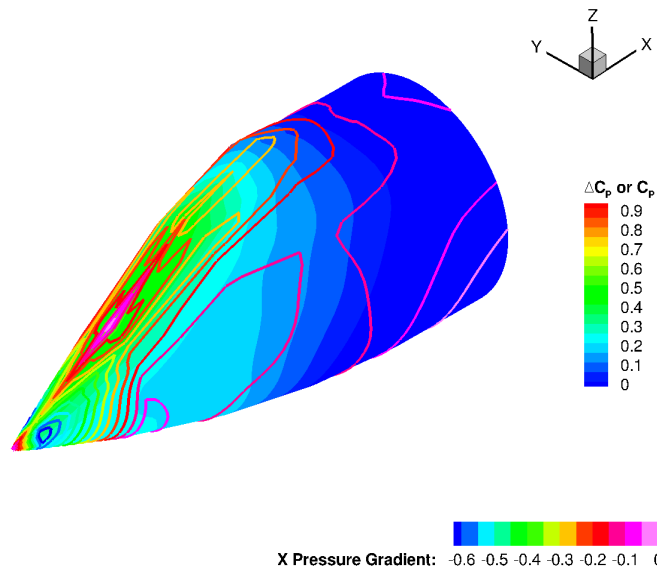


Figure 14. X – pressure gradients.

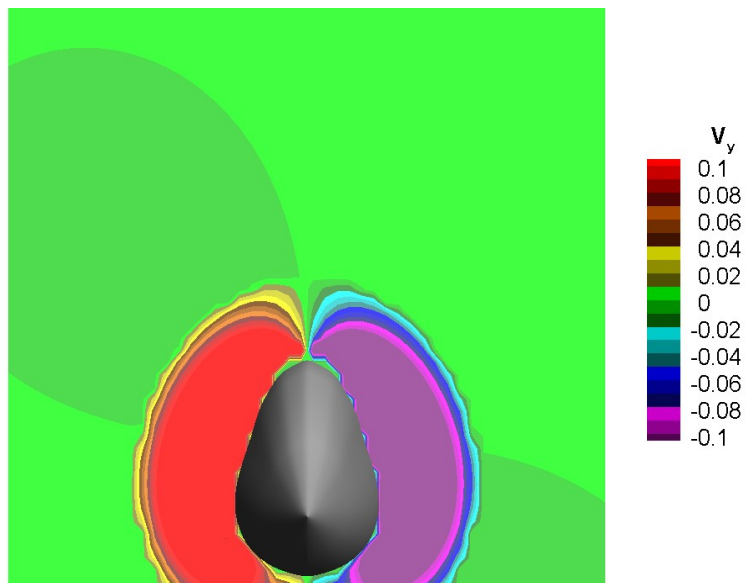


Figure 15. Y – velocity field.

The second methodology is using the Best Practice eXpert System which is a GUI-application based on a knowledge database which provides user guidance to the CFD process. The following figure is a sample screenshot pertaining to missile body configuration at supersonic speeds.

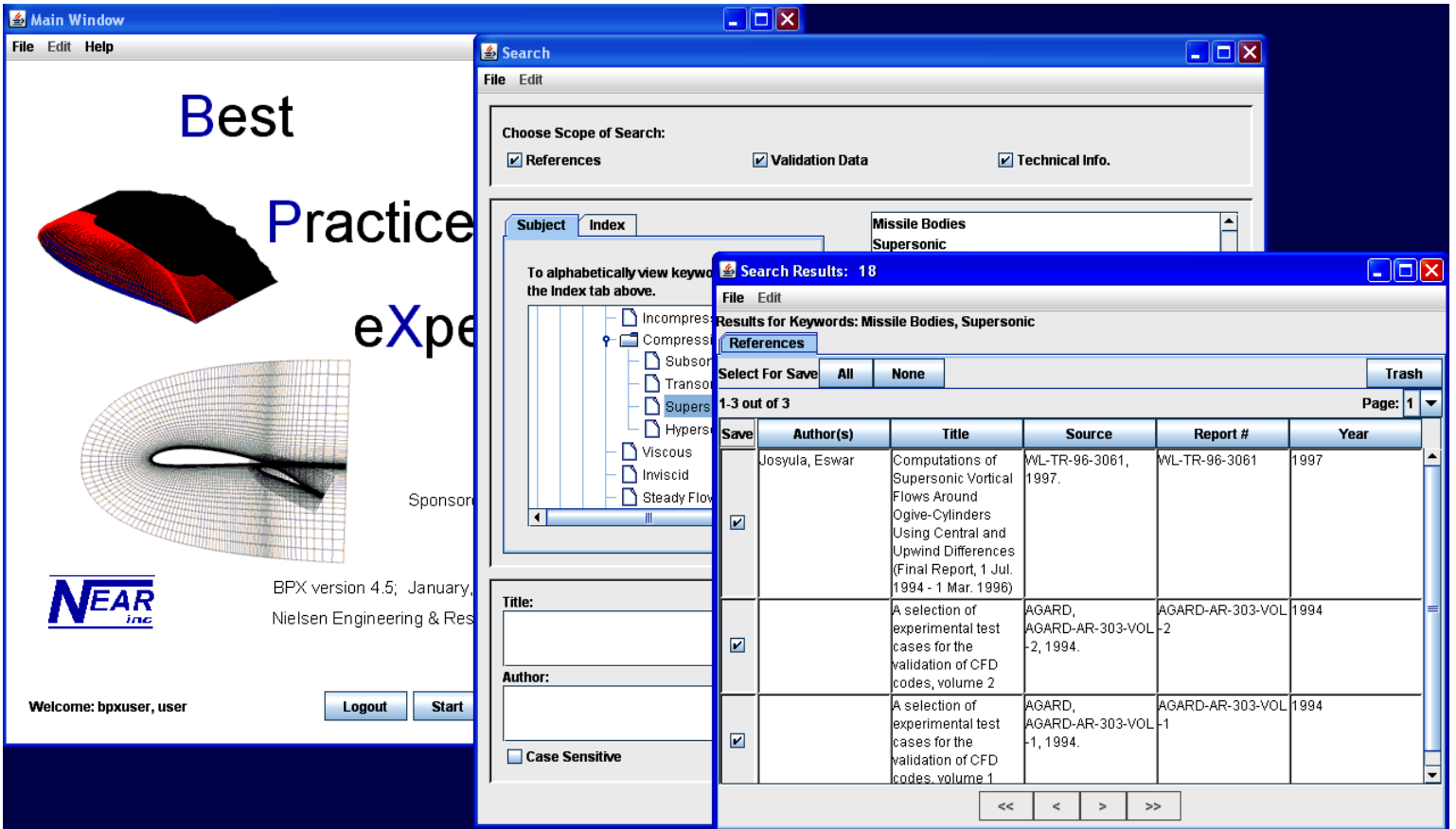


Figure 16. BPX GUI

As one can observe, the keywords Missile Bodies and Supersonic output 3 search results that the user can use to obtain further knowledge on the type of problem, grid topology, and grid resolution.

The third methodology is more automated; the user defines an initial-spacing, end-spacing, and Δs ratio. AeroAssist will use the information gathered from the pressure gradient to distribute, add, or remove points. The purpose is to increase the resolution in areas of high-pressure gradients and decrease resolution in areas of low-pressure gradients to avoid numerical diffusion, save time, and computational expense.

AeroAssist, with the help of SAGE (Self Adaptive Grid Code), adds and redistributes the point accordingly to redefine the surface mesh. The following is the SAGE input code to generate Figure 24 and 25:

- *\$name1 reclust=1,mvbound=0,dsw=0.005,dse=1,indq=6,save=.f. \$ (fig 24)*
- *\$name1 add=1,lstadd=15,lendadd=51,indq=6,save=.f. \$ (fig 24)*
- *\$name1 reclust=1,mvbound=0,dsw=0.005,dse=1,indq=6 \$ (fig 24)*
- *\$name1 add=2,rdsmax=1.0,reclust=1,mvbound=0,indq=6 \$ (fig 25)*

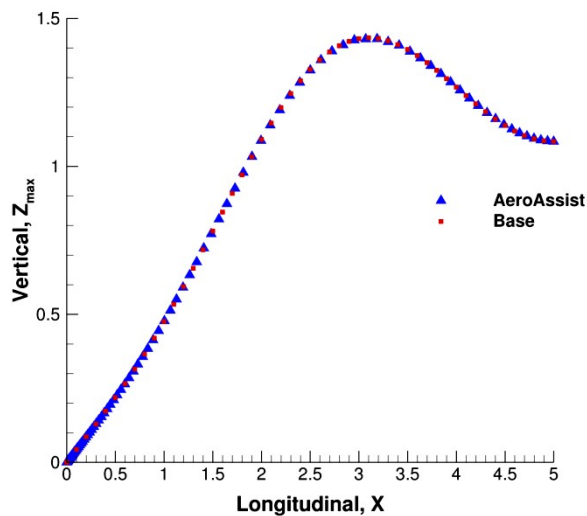


Figure 17. Streamwise resolution refinement.

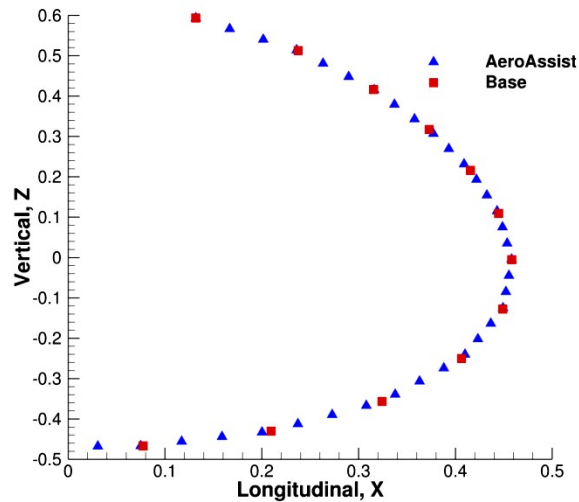


Figure 18. Circumferential resolution refinement.

Based on best practices and the flow feature extraction module, the streamwise direction is modified by adding a constraint at the leading edge of the nose and the end of the body due to the boundary condition; points are added and distributed accordingly. The old geometry represented by pink dots (Figure 26) was defined by 51 points. The new geometry represented by green dots (Figure 24) is now 84 points. In the circumferential direction there are not many changes occurring; however, due to the symmetrical boundary condition there is a small constraint defined by BPX. The old geometry represented by pink dots (Figure 25) was defined by 13 points. The new geometry represented by the green dots (Figure 25) is now 37 points.

With the output from the Information Layer an intelligent surface grid is generated based on mesh metrics, mesh quality, and physics. The new surface grid is composed of 3,305 cells which is less than the first generation grid shown in Figure 15.

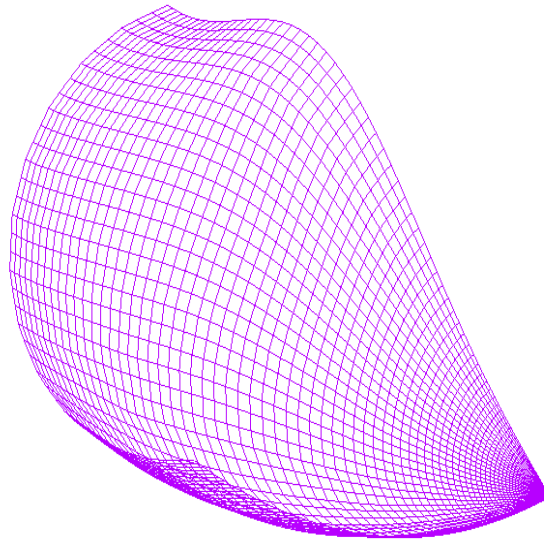


Figure 19: AeroAssist surface grid.

G. VOLUME GENERATION

It is not enough to conclude that a better surface grid has been created without actually solving the flow around it. With the help of AeroAssist, it was determined that the maximum normal distance to grow the volume grid had to be approximately 6 units.

For the volume generation in Figure 29: the computational domain does not extend downstream beyond the length of the forebody; however it extends to 6 characteristic length (L) in the radial direction. The volume mesh was created from the extrusion of the surface in the radial direction and creating linear lines from the inner to the outer surface. This then enables the option to create edges to construct many faces, and for every 6 faces a block was generated, creating the volume over the surface. This grid had a total of 283,388 cells.

For the volume generation in Figure 31: the computational volume was generated

using a hyperbolic grid generator, hypgen, to maintain orthogonality and appropriate ratio spacing of less than 1.2. The following figures are a comparison between the first generation volume grid (manually designed) and the hyperbolic volume grid from the AeroAssist surface grid. This grid had a total of 198,144 cells, which is approximately a 43% saving on number of cells. This saving will not only convert into computational time, but also the assisted volume grid is viscous and it extends further in the upstream direction.

The following input was used to create the computational volume for Figure 31:

```

grid2d.dat
grid3d.dat
0                IFORM(0/1)
1, 1, 3         IZSTRT(1/1/1),NZREG,KLAYER
65, 6.0, 5e-5, 0 NPZREG(),ZREG(),DZ0(),DZ1()
20, -1, 2, 2    IBCJA,IBCJB,IBCKA,IBCKB
1, 0.00, 4, 2  IVSPEC(1/2),EPSSS,ITSVOL,NSUB
1, 0.8         IMETH(0/2/3),SMU2
0.0, 0.0      TIMJ,TIMK
1, 0.50, 0.60 IAXIS(1/2),EXAXIS,VOLRES

```

The total number of points in the I,J, K direction are the following:

<u>#Cells =</u>	<u>#Cells =</u>
<u>283,388</u>	<u>198,144</u>
<i>I = 142</i>	<i>I = 87</i>
<i>J = 70</i>	<i>J = 37</i>
<i>Z = 30</i>	<i>Z = 65</i>

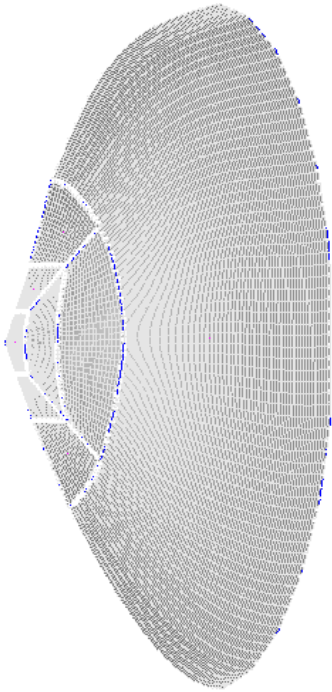


Figure 20: ESI geom volume grid.

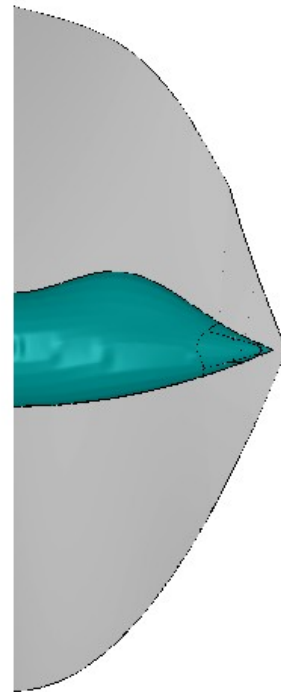


Figure 21: ESI volume side view.

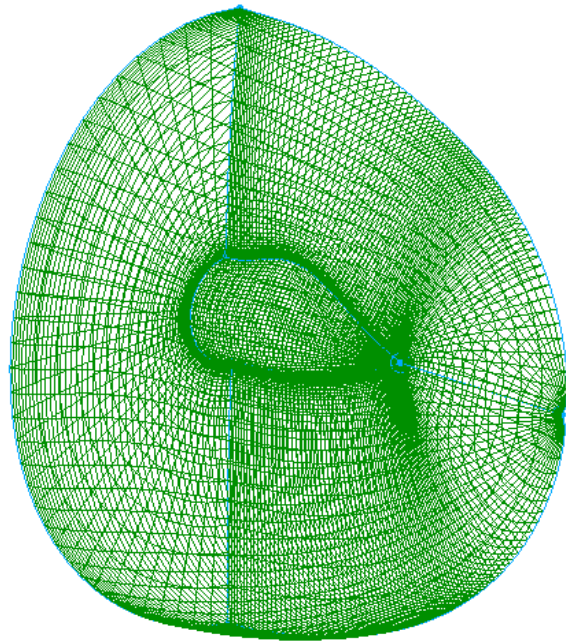


Figure 22: AeroAssist - hypgen volume grid

H. CODE COMPARISON

Now that the geometry has been obtained, it is important to verify the solution with respect to the experimental data. In order to do so, the CFD code OVERFLOW was chosen, even though, the previous solution was done using ESI Suite. The reason being was the ease and the one-to-one comparison no longer existed because the previous solution was inviscid. Hence, the solution will be distinct either using ESI or OVERFLOW. To assess the comparison between the codes, the residual history and the mach contour will be shown. More information about these codes can be obtained in the Appendix F and H sections.

Boundary Condition:

- ESI
 - Model Options (MC): Inviscid Flow.
 - Plane of Symmetry ($y = 0$).
 - Inlet Conditions (IC): Fixe Mass Flow Rate.
 - Outlet Conditions (OC): Extrapolated.
- Overflow
 - Viscous adiabatic wall.
 - Plane of Symmetry($y=\text{constant}$).
 - Riemann invariants with freestream imposed characteristics.
 - Outflow (pure extrapolation).

Residual Plot:

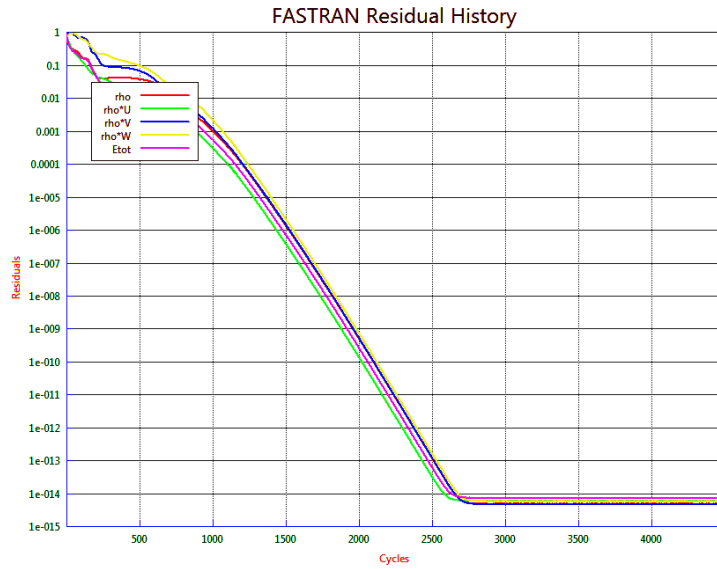


Figure 23: ESI residual history.

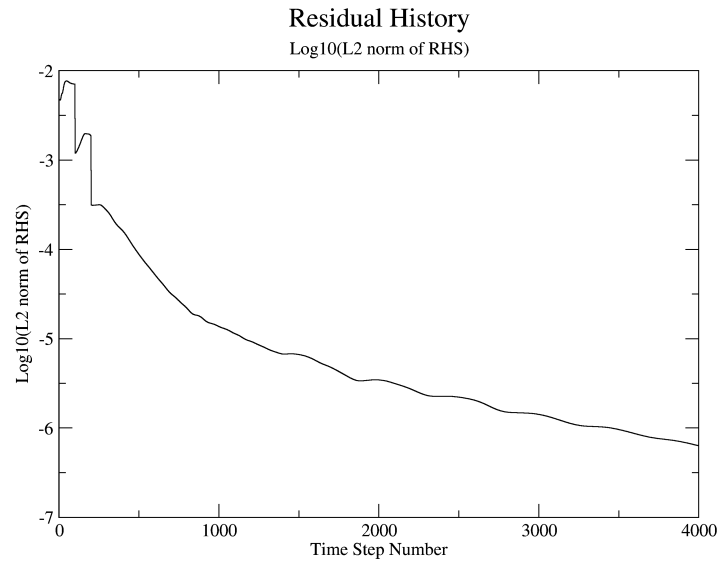


Figure 24: Overflow residual history.

The overall residual plots show at least 4 orders of magnitude in error reduction. Best practices suggest that a drop of 3–5 orders or magnitude is good enough.

Mach Contours:

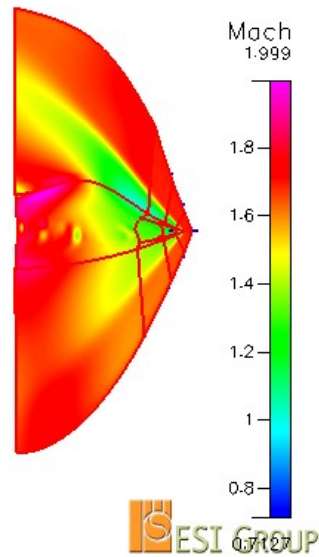


Figure 25: ESI Mach sideview result.

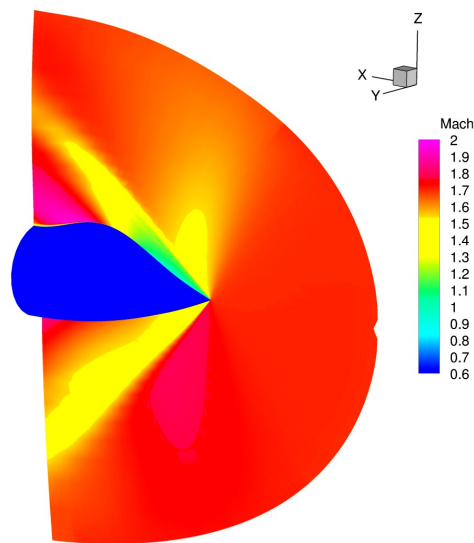


Figure 26: Overflow Mach isometric view result.

Both solutions have similar Mach contours and capture the shock. The shock effect causes the viscous forces to have a locally negligible influence. However, it is clear that OVERFLOW is a viscous solution due to the no-slip condition at the body surface.

I. BENCHMARK

The computations were done using the pressure results from CFD-View and Excel (a sample calculation can be seen in Appendix H). The benchmark was done for θ at 2 angles: 0° and 180° , where θ is the azimuthal variable defined in the figure below:

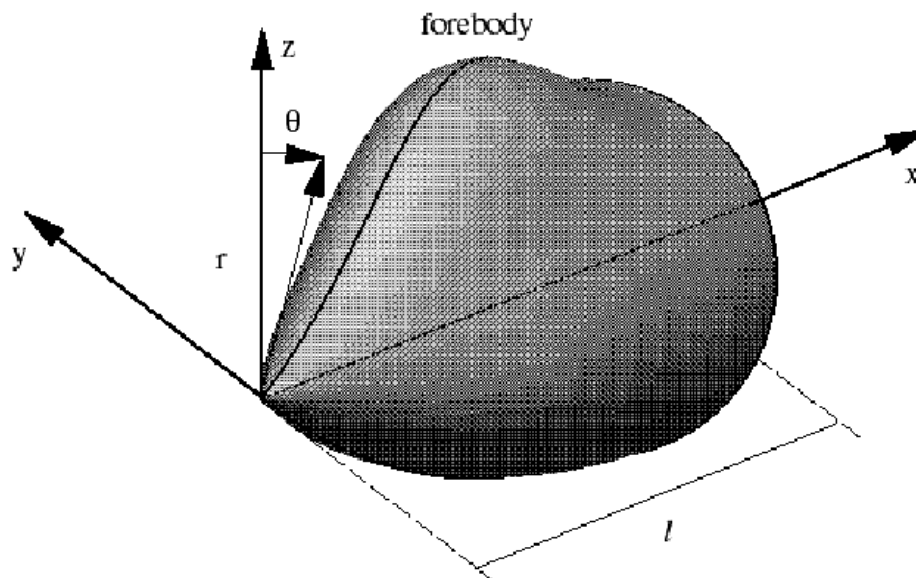


Figure 27: Polar coordinate system.

As θ rotates the pressures values are obtained in the yz – plane along the characteristic length of the forebody. The pressure coefficient (C_p) is determined for each point where the pressure values are taken; as a result, a plot of C_p vs. x/l for each value of θ is determined and compared to the published experimental results. The following are the graphs comparison of the CFD results with respect to the published data.

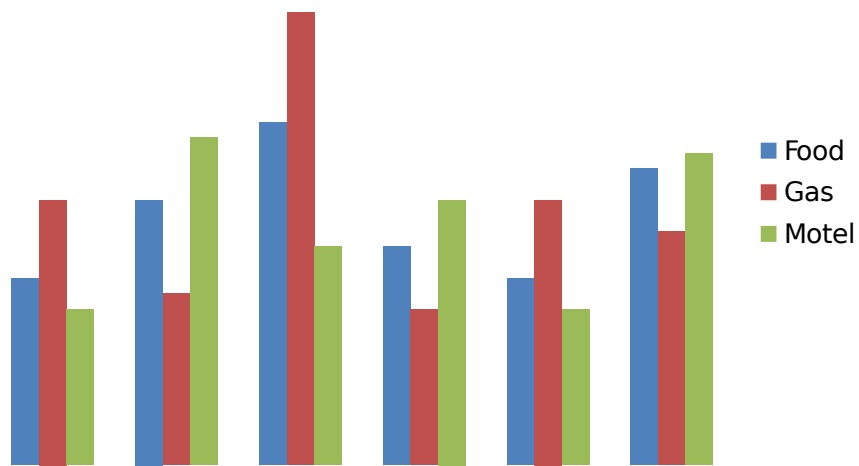


Figure 28: Pressure distribution comparison.

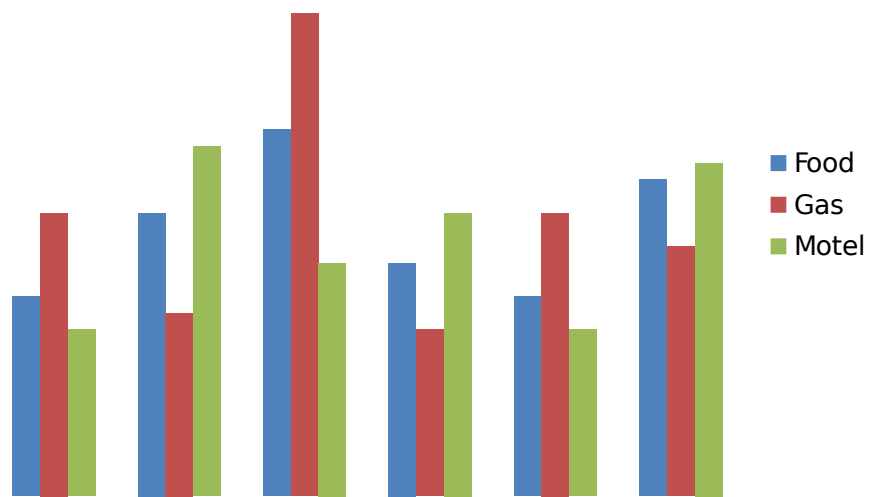


Figure 29: Pressure distribution comparison.

Due to the shock effect, the pressure coefficient variation is minimal. However, for $\theta=180^\circ$ the OVERFLOW data coincides with the experimental data.

V. CONCLUSION

The balance between physical fidelity and computational expense is a problem that CFD practitioners usually must address through intuition and experience. AeroAssist is a tool that can bridge the gap between the user's inexperience and knowledge by providing physics based solutions to aid in the generation of economical and quality surface grids.

Anticipated improvements in surface grid generation will be of immediate use where conventional CFD grid generation has its deficiencies. The work done proves the viability and fundamental parameters to produce an independent grid generation guide tool, AeroAssist, capable of creating more "accurate" computational mesh(es).

VI. VISION

Ultimately, a GUI platform will integrate *a priori* solutions of the geometry of interest, uncertainty and error analysis, expert system knowledge, and a database management system.

The continuing effort and development will enhance AeroAssist by including unstructured grid elements, and the integration of mesh quality/resolution practices for different flow solvers such as Overflow, TetrUSS, FLUENT, CFX, STAR CCM+, etc. In addition, a module will be developed to identify and quantify uncertainty due to the geometrical properties and solution. AeroAssist will also integrate a database management system.

The formulation of a software development plan will include the identification of a suitable architecture, platform, and computer language. This effort will lead to the development of an AeroAssist GUI (Figure 39).

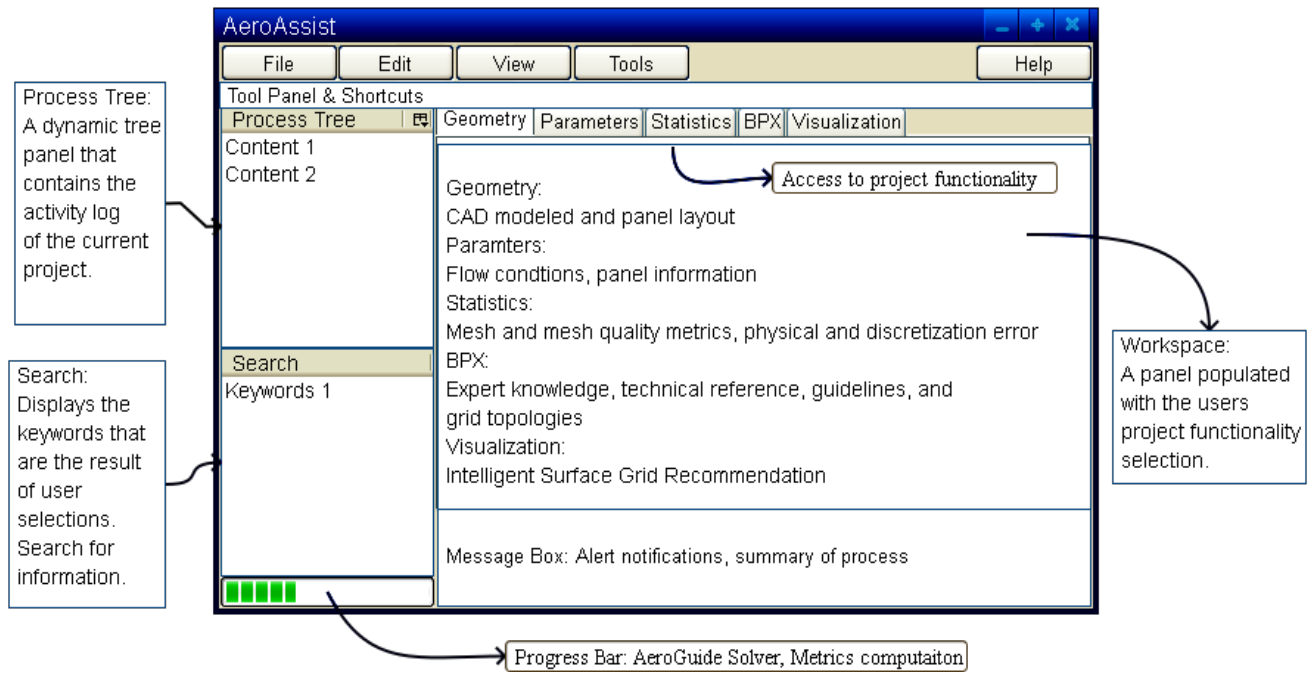


Figure 1 Conceptual GUI.

Other areas of research would be:

- Recommendations for an optimum topology for a range of flow conditions.
- Development of a dynamic system where the user can visualize the deformation of the recommended grid based on uncertainty and flow conditions.
- Capability of inputting previously developed grids into AeroAssist to evaluate the mesh metrics and mesh quality metrics.

VII.

VIII. REFERENCES

¹Roy, C.J., “Review of Discretization Error Estimators in Scientific Computing.” AIAA 2010-126, American Institute of Aeronautics and Astronautics, Reston, VA, January 2010.

²Shih, A., Ito, Y., Koomullil, R., Kasmai, T., Jankun-Kelly, M., Thompson, D., and Brewer, D., “Solution Adaptive Mesh Generation using Feature-Aligned Embedded Surface Meshes,”” AIAA 2007-558, American Institute of Aeronautics and Astronautics, Reston, VA, January 2007.

³Dillenius, M. F. E., Lesieutre, D. J., Hagedus, M. C., Perkins, S. C., Jr., Love, J. F., and Lesieutre, T. O., “Engineering-, -Intermediate – and High-Level Aerodynamic Prediction Methods and Applications,” Journal of Spacecraft and Rockets, Vol. 36, No. 5, Sep.-Oct. 1999, pp. 609-620.

⁴Stremel, P. M., Mendenhall, M. R., and Hagedus, M. C., “BPX – A Best Practices Expert System for CFD,” AIAA 2007-974, Jan. 2007.

⁵Knupp, P., “Remarks on Mesh Quality,” AIAA 2008-933, American Institute of Aeronautics and Astronautics, Reston, VA, Jan. 2008.

⁶Marviplis, D.J., et al., “Grid Quality and Resolution Issues from the Drag Prediction Workshop Series,” AIAA-2008-0930, Jan. 2008.

⁷ Gatt Engineering Consultants, “Significance of CFD Analysis in Modern Industry,” proceedings on the website <http://cfdanalysisisservices.net/cfd-analysis-services-significance-of-cfd-analysis-in-modern-industry/>.

⁸Petersson, A.N., “A Software Demonstration of ‘rap’:Preparing CAD geometries for Overlapping Grid Generation,” Report UCRL-JC-147260, Lawrence Livermore National Laboratory, 2002.

⁹Haimes, R., “Final Report for NAG1-0204, CAPRI: A Geometric

Foundation for Computational Analysis and Design,” Document ID 20070022429, National Aeronautics and Space Administration, NASA Langley Research Center, VA, Oct. 2006

¹⁰Dawes, W.N., “Turbomachinery Computational Fluid Dynamics: Asymptotes and Paradigm Shifts,” Department of Engineering, University of Cambridge, May 2007.

¹¹Tomac, M., Rizzi, A., and Ooppelstrup, J., “From Geometry to CFD Grids – An Automated Approach for Conceptual Design,” AIAA 2010-8240, American Institute of Aeronautics and Astronautics, Reston, VA, Aug. 2010.

¹²Chan, W.M., “Developments in Strategies and Software Tools for Overset Structured Grid Generation and Connectivity,” AIAA 2011-3051, American Institute of Aeronautics and Astronautics, Reston, VA, Jun. 2011.

¹³Thornburg, H.J., “Overview of the PETTT Workshop on Mesh Quality/Resolution, Practice, Current Research, and Future Directions,” AIAA 2012-0606, American Institute of Aeronautics and Astronautics, Reston, VA, Jan. 2012.

¹⁴Han, D. and Hosder, S., “Inherent and Model-Form Uncertainty Analysis for CFD Simulation of Synthetic Jet Actuators,” AIAA-2012-0082.

¹⁵ESI CFD, Inc., “Supersonic Forebody Validation,” CFD-FASTRAN Dem/Val Manual, 2004.

¹⁶Anderson, J.D., “Modern Compressible Flow,” 3rd ed., McGraw Hill, New York, 2003.

¹⁷Davies, C.B., “SAGE, The Self-Adaptive Grid code”, Version 4, Eloret Corp.

IX. APPENDIX

A. AERODYNAMIC MODELING AND PREDICTION CAPABILITIES

Panel method-based aerodynamic prediction methods developed by NEAR, such as *OPTMIS/MISDL* are very versatile and have been successfully used to model a variety of flight vehicles including, missiles, aircraft, UAV's, bodies, wings, strongly cambered hydrodynamic depressors. Important modeling and capabilities of the methodology include nonlinear phenomena associated with Mach number, angle of attack and sideslip, fin and control surface deflections and vortex effects including swirling flow. Empirical databases of airfoil sectional properties as part of a stall model and improved drag prediction. The ability of this code to model and estimate and identify important flow phenomena such as separation, shock waves, vortical structures, etc. is critical to an intelligent tool to aid the grid design process. These methods can also perform hundreds of analyses in a matter minutes which permits a whole range of flight conditions to be investigated to help assess when a new or modified grid would be required by CFD in order to obtain more accurate results.

B. BEST PRACTICES EXPERT FOR CFD

Michael Mendenhall of NEAR led the development of a Best Practice eXpert system for CFD (BPX).⁴ This effort involved melding the art and science involved with obtaining accurate CFD grids and solutions. The art involves CFD experience and engineering diligence, and the science entails specific guidelines and checklists. The

goals of this effort and the tool BPX include: consistent high-quality solutions, uncertainty reduction, error minimization, more efficient cfd tools, lower cost, elimination of unnecessary runs, no repetition of past mistakes, and leveraging of corporate and expert knowledge. The BPX is a bridge between the art and science of CFD and will be used as an integral part of the proposed AeroAssist tool for and quality grid generations.

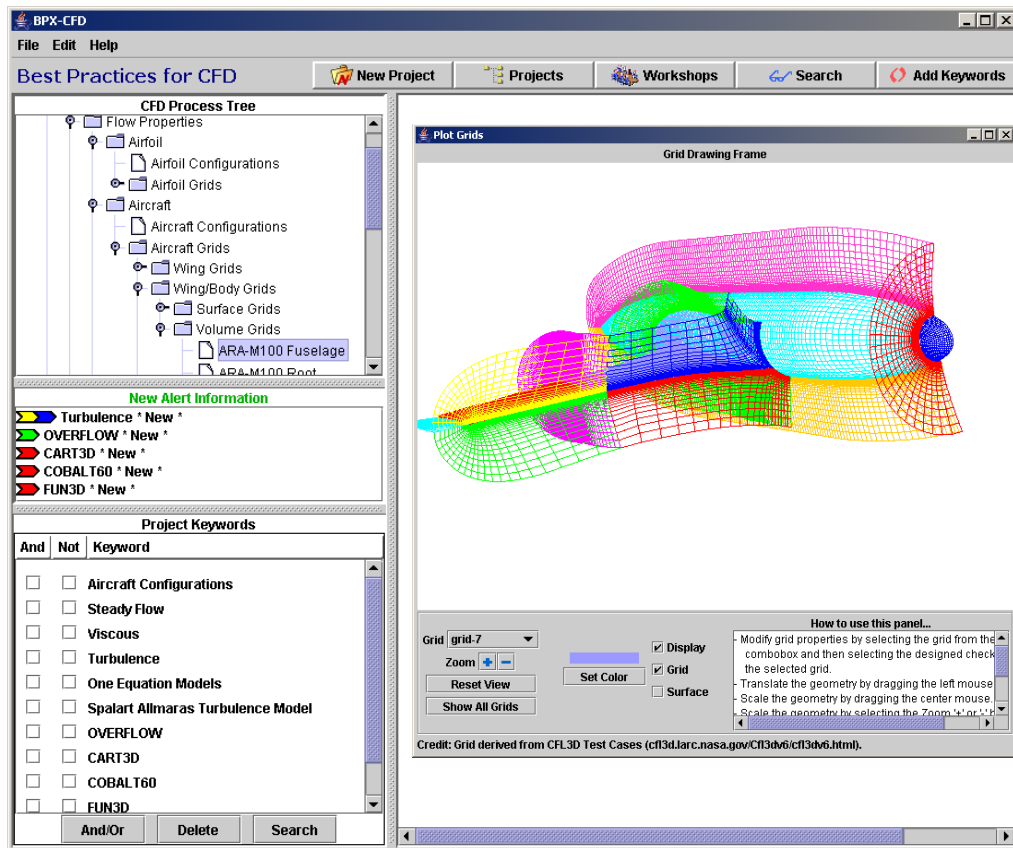


Figure 1 BPX GUI.

C. MESH AND QUALITY METRICS NUMERICS

Solution-adaptive grid methods are useful tools for efficient and accurate flow solutions in certain regions of the flow. It is obvious that the greater the number of points

in the computational mesh, the more accurate the numerical solution will be.¹⁷ However, an over-defined computational mesh can introduce other errors and create instability. The SAGE code, Self-Adaptive Grid Code, adds and redistributes the points in regions of strong flow gradients and disperses them in region of weak flow gradients. The code accommodates two-dimensional, three-dimensional, finite-difference and finite-volume, single grid and zonal-matching multiple grid flow.¹⁷ It was developed by Carol B. Davies at NASA/AMES and it will be an integral part of AeroAssist.

D. OPTIMIZATION AND UNCERTAINTY QUANTIFICATION

In recent years, NEAR has been actively involved in developing and demonstrating critical technologies for multipoint, multidisciplinary, and multifidelity design optimization including the incorporation of uncertainty and risk. The uncertainty and sensitivity analysis of this work has direct relevance to the AeroAssist tool capabilities. Dr. Reisenhel of NEAR, is the developer of multidimensional response surface technology which has been an enabler for risk-based and multifidelity unsteady design-optimization. He has applied sequential radial basis function surrogate-based optimization techniques for aeroelastic wing design and developed efficient global search methods based on Multi-Fidelity Expected Improvement concepts. Furthermore, Dr. Reisenhel examined the trade-off between initial DOE and subsequent optimization-based in-fills of sequential surrogate-based optimization

E. POINTWISE

Pointwise is a software for generating CFD meshes: structured, unstructured, and hybrid grids. In addition, Pointwise Native CAD Readers can be used to read geometry in its native format.

F. ESI

ESI offers a variety of multiphysics solvers. CFD-GEOM is the grid generation system. It allows the user to manipulate CAD models, and supports the python scripting language. CFD-Fastran, the solver used in this project, simulates and analyses problems dealing with high-speed flows. It supports all grid technologies including multi-block structured, general polyhedral unstructured, chimera/overset and adaptive Cartesian. CFD-VIEW lets the user visualize the flow physics, animate transient data sets, and extract data relevant to engineering design.

G. HYPGEN

Hypgen is a program used to generate a volume grid over a user-supplied surface grid in three dimensions. It is part of the Chimera Grid Tools, and it is intended for overset field grid generation on complex geometries.

H. OVERFLOW

The NASA code OVERFLOW is a three-dimensional time-marching implicit Navier-Stokes flow solver that operates on structured overset grids. It has several different

inviscid flux algorithms, implicit solution algorithms, and options for thin layer or full viscous terms.

I. TECPLOT

Tecplot 360 is a CFD visualization software tool with multiple loaders that helps you plot and animate a solution set, analyze complex data, and communicate the results.

J. SAMPLE RAW DATA

Table 2. Sample raw data for one curve at $\psi = 6.25$.

r_1	ψ	r_2	l	L	y/L	z/L	x	y	z	PC
0.998 9	6.250 0	0.044 3	1.000 0	1.000 0	0.001 5	0.044 4	0.020 0	0.001 5	0.044 4	1
0.998 9	6.250 0	0.087 7	1.000 0	1.000 0	0.002 9	0.088 6	0.040 0	0.002 9	0.088 6	2
0.998 9	6.250 0	0.130 2	1.000 0	1.000 0	0.004 4	0.133 3	0.060 0	0.004 4	0.133 3	3
0.998 9	6.250 0	0.171 8	1.000 0	1.000 0	0.005 8	0.179 1	0.080 0	0.005 8	0.179 1	4
0.998 9	6.250 0	0.212 5	1.000 0	1.000 0	0.007 3	0.226 6	0.100 0	0.007 3	0.226 6	5
0.998 9	6.250 0	0.252 4	1.000 0	1.000 0	0.008 8	0.276 1	0.120 0	0.008 8	0.276 1	6
0.998 9	6.250 0	0.291 3	1.000 0	1.000 0	0.010 3	0.328 0	0.140 0	0.010 3	0.328 0	7
0.998 9	6.250 0	0.329 3	1.000 0	1.000 0	0.011 8	0.382 5	0.160 0	0.011 8	0.382 5	8
0.998	6.250	0.366	1.000	1.000	-	0.439	0.180	-	0.439	9

9	0	4	0	0	0.013 4	7	0	0.013 4	7	
0.998 9	6.250 0	0.402 7	1.000 0	1.000 0	- 0.015 0	0.499 6	0.200 0	- 0.015 0	0.499 6	1
0.998 9	6.250 0	0.438 0	1.000 0	1.000 0	- 0.016 6	0.562 1	0.220 0	- 0.016 6	0.562 1	1
0.998 9	6.250 0	0.472 5	1.000 0	1.000 0	- 0.018 2	0.626 8	0.240 0	- 0.018 2	0.626 8	1
0.998 9	6.250 0	0.506 0	1.000 0	1.000 0	- 0.019 9	0.693 5	0.260 0	- 0.019 9	0.693 5	1
0.998 9	6.250 0	0.538 7	1.000 0	1.000 0	- 0.021 6	0.761 7	0.280 0	- 0.021 6	0.761 7	1
0.998 9	6.250 0	0.570 5	1.000 0	1.000 0	- 0.023 2	0.830 9	0.300 0	- 0.023 2	0.830 9	1
0.998 9	6.250 0	0.601 3	1.000 0	1.000 0	- 0.024 9	0.900 4	0.320 0	- 0.024 9	0.900 4	1
0.998 9	6.250 0	0.631 3	1.000 0	1.000 0	- 0.026 6	0.969 5	0.340 0	- 0.026 6	0.969 5	1
0.998 9	6.250 0	0.660 4	1.000 0	1.000 0	- 0.028 2	1.037 6	0.360 0	- 0.028 2	1.037 6	1
0.998 9	6.250 0	0.688 6	1.000 0	1.000 0	- 0.029 7	1.103 9	0.380 0	- 0.029 7	1.103 9	1
0.998 9	6.250 0	0.715 9	1.000 0	1.000 0	- 0.031 2	1.167 7	0.400 0	- 0.031 2	1.167 7	2
0.998 9	6.250 0	0.742 3	1.000 0	1.000 0	- 0.032 7	1.228 2	0.420 0	- 0.032 7	1.228 2	2
0.998 9	6.250 0	0.767 8	1.000 0	1.000 0	- 0.034 0	1.284 7	0.440 0	- 0.034 0	1.284 7	2
0.998 9	6.250 0	0.792 4	1.000 0	1.000 0	- 0.035	1.336 6	0.460 0	- 0.035	1.336 6	2

					3			3		
0.998 9	6.250 0	0.816 1	1.000 0	1.000 0	0.036 5	1.383 3	0.480 0	0.036 5	1.383 3	2
0.998 9	6.250 0	0.838 9	1.000 0	1.000 0	0.037 5	1.424 3	0.500 0	0.037 5	1.424 3	2
0.998 9	6.250 0	0.860 9	1.000 0	1.000 0	0.038 5	1.459 1	0.520 0	0.038 5	1.459 1	2
0.998 9	6.250 0	0.881 9	1.000 0	1.000 0	0.039 3	1.487 5	0.540 0	0.039 3	1.487 5	2
0.998 9	6.250 0	0.902 0	1.000 0	1.000 0	0.040 0	1.509 3	0.560 0	0.040 0	1.509 3	2
0.998 9	6.250 0	0.921 3	1.000 0	1.000 0	0.040 6	1.524 3	0.580 0	0.040 6	1.524 3	2
0.998 9	6.250 0	0.939 6	1.000 0	1.000 0	0.041 0	1.532 6	0.600 0	0.041 0	1.532 6	3
0.998 9	6.250 0	0.957 1	1.000 0	1.000 0	0.041 3	1.534 3	0.620 0	0.041 3	1.534 3	3
0.998 9	6.250 0	0.973 6	1.000 0	1.000 0	0.041 5	1.529 7	0.640 0	0.041 5	1.529 7	3
0.998 9	6.250 0	0.989 3	1.000 0	1.000 0	0.041 6	1.519 2	0.660 0	0.041 6	1.519 2	3
0.998 9	6.250 0	1.004 0	1.000 0	1.000 0	0.041 6	1.503 3	0.680 0	0.041 6	1.503 3	3
0.998 9	6.250 0	1.017 9	1.000 0	1.000 0	0.041 5	1.482 6	0.700 0	0.041 5	1.482 6	3
0.998 9	6.250 0	1.030 9	1.000 0	1.000 0	0.041 3	1.457 7	0.720 0	0.041 3	1.457 7	3
0.998 9	6.250 0	1.043 0	1.000 0	1.000 0	0.041 0	1.429 4	0.740 0	0.041 0	1.429 4	3

0.998 9	6.250 0	1.054 2	1.000 0	1.000 0	- 0.040 7	1.398 5	0.760 0	- 0.040 7	1.398 5	3
0.998 9	6.250 0	1.064 4	1.000 0	1.000 0	- 0.040 3	1.365 9	0.780 0	- 0.040 3	1.365 9	3
0.998 9	6.250 0	1.073 8	1.000 0	1.000 0	- 0.039 9	1.332 3	0.800 0	- 0.039 9	1.332 3	4
0.998 9	6.250 0	1.082 3	1.000 0	1.000 0	- 0.039 5	1.298 7	0.820 0	- 0.039 5	1.298 7	4
0.998 9	6.250 0	1.089 9	1.000 0	1.000 0	- 0.039 1	1.266 0	0.840 0	- 0.039 1	1.266 0	4
0.998 9	6.250 0	1.096 7	1.000 0	1.000 0	- 0.038 7	1.234 9	0.860 0	- 0.038 7	1.234 9	4
0.998 9	6.250 0	1.102 5	1.000 0	1.000 0	- 0.038 3	1.206 2	0.880 0	- 0.038 3	1.206 2	4
0.998 9	6.250 0	1.107 4	1.000 0	1.000 0	- 0.038 0	1.180 6	0.900 0	- 0.038 0	1.180 6	4
0.998 9	6.250 0	1.111 4	1.000 0	1.000 0	- 0.037 7	1.158 8	0.920 0	- 0.037 7	1.158 8	4
0.998 9	6.250 0	1.114 6	1.000 0	1.000 0	- 0.037 4	1.141 3	0.940 0	- 0.037 4	1.141 3	4
0.998 9	6.250 0	1.116 8	1.000 0	1.000 0	- 0.037 3	1.128 4	0.960 0	- 0.037 3	1.128 4	4
0.998 9	6.250 0	1.118 1	1.000 0	1.000 0	- 0.037 1	1.120 6	0.980 0	- 0.037 1	1.120 6	4
0.998 9	6.250 0	1.118 6	1.000 0	1.000 0	- 0.037 1	1.118 0	1.000 0	- 0.037 1	1.118 0	5

K. ESI SAMPLE CALCULATION

Sample Calculation of C_p vs. x/l

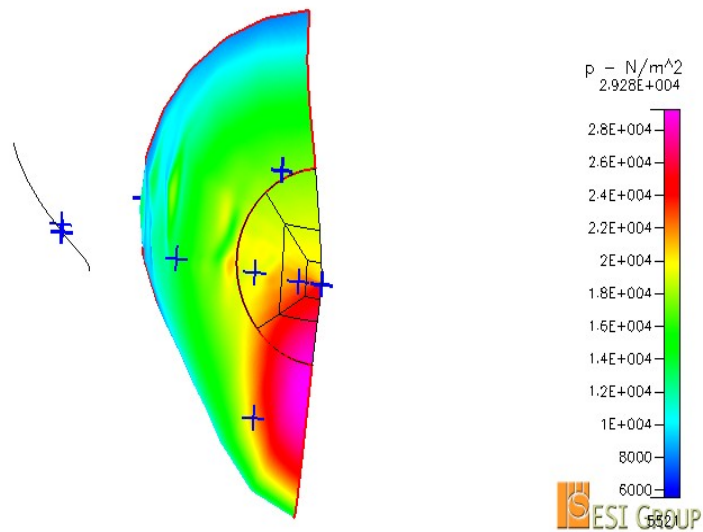


Figure 30: Pressure distribution for $\theta = 180^\circ$.

Table 3. ESI data extraction for $\theta = 180^\circ$.

$\theta = 180$				
P inf (Kpa)	P (KPa)	q inf (Kpa)	x/l	C_p
11.4	16.861	23.1	0	0.236407
	19.327		0.1	0.34316
	18.329		0.2	0.299957
	17.154		0.3	0.249091
	15.707		0.4	0.18645
	14.107		0.5	0.117186
	12.254		0.6	0.03697
	10.566		0.7	-0.0361
	9.285		0.8	-0.09156
	8.574		0.9	-0.12234
	8.234		1	-0.13706

C_p value at $x/l = 0$

$$C_p = \frac{P - P_\infty}{q_\infty} = \frac{16.861 - 11.4}{23.1} = 0.236407$$

L. OVERFLOW DATA EXTRACTION

Table 4. OVERFLOW data extraction for $\theta=180^\circ$

x/l	Cp		x/l	Cp		x/l	Cp
0	0.473594		0.133062	0.232314		0.773511	-0.01757
0.000906	0.300267		0.142533	0.224796		0.793306	-0.02567
0.001878	0.308477		0.152539	0.218829		0.812626	-0.0341
0.00292	0.315156		0.163078	0.212777		0.831444	-0.04244
0.004037	0.316777		0.174176	0.20568		0.849728	-0.05016
0.005236	0.316449		0.185844	0.198917		0.867454	-0.0575
0.00652	0.31577		0.198091	0.189801		0.884603	-0.06474
0.007897	0.315765		0.21094	0.18227		0.901158	-0.07216
0.009373	0.316063		0.224387	0.173833		0.917112	-0.07974
0.010955	0.316046		0.238444	0.165264		0.932454	-0.08622
0.012649	0.315533		0.253117	0.159293		0.947185	-0.09115
0.014463	0.315466		0.268397	0.151963		0.961296	-0.0975
0.016406	0.316778		0.284283	0.142074		0.974802	-0.10427
0.018487	0.314875		0.300771	0.132221		0.987701	-0.10697
0.020715	0.305084		0.317855	0.124189		1	-0.10697
0.023105	0.300624		0.335517	0.117096			
0.02566	0.302447		0.353736	0.110335			
0.028393	0.302106		0.372487	0.103171			
0.031315	0.302248		0.391747	0.095441			
0.034436	0.302537		0.411482	0.087654			
0.037771	0.299522		0.43166	0.080627			
0.041335	0.291159		0.452234	0.075185			
0.045148	0.2865		0.473165	0.069481			
0.049216	0.286971		0.494399	0.063593			
0.053552	0.286146		0.515899	0.05822			
0.058173	0.282814		0.537577	0.052548			
0.063102	0.27716		0.559431	0.047004			
0.068355	0.275573		0.581369	0.041298			
0.073941	0.275228		0.60335	0.035275			
0.079879	0.266942		0.625291	0.029619			
0.086207	0.260333		0.647154	0.023711			
0.092922	0.259419		0.668877	0.017255			
0.100043	0.253834		0.690404	0.011249			
0.107608	0.249132		0.711683	0.004686			
0.115615	0.245789		0.732655	-0.00264			
0.124093	0.238141		0.753281	-0.00992			

M. EXPERIMENTAL DATA

Graph of C_p vs. x/l for $\theta=180^\circ$

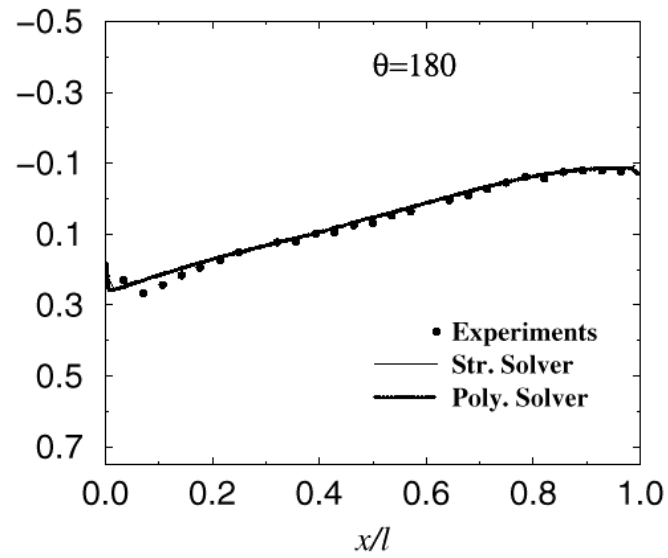


Figure 31. Experimental results for $\theta = 180^\circ$.

Table 5. Experimental data extraction for $\theta = 180^\circ$.

x/l	Cp		x/l	Cp		
0.034653	0.226935		0.749175	-0.04799		
0.070957	0.264087		0.783828	-0.06285		
0.110561	0.241796		0.820132	-0.06037		
0.141914	0.209598		0.853135	-0.07771		
0.179868	0.19226		0.892739	-0.08266		
0.214521	0.174923		0.925743	-0.08266		
0.247525	0.147678		0.965347	-0.07523		
0.320132	0.12291					
0.353135	0.11548					
0.394389	0.095666					
0.429043	0.090712					
0.462046	0.070898					
0.50165	0.063467					
0.537954	0.043653					
0.572607	0.033746					
0.638614	-0.00341					
0.678218	-0.01331					
0.714521	-0.03065					